Bioelectrochemistry 135 (2020) 107574

Contents lists available at ScienceDirect

Bioelectrochemistry

journal homepage: www.elsevier.com/locate/bioelechem

NAD(P)-dependent glucose dehydrogenase: Applications for biosensors, bioelectrodes, and biofuel cells

Krzysztof Stolarczyk [a], Jerzy Rogalski [b], Renata Bilewicz [a,*]

[a] Faculty of Chemistry, University of Warsaw, Pasteura St. 1, 02-093 Warsaw, Poland
[b] Department of Biochemistry and Biotechnology, Maria Curie-Sklodowska University, Akademicka Str. 19, 20-031 Lublin, Poland

ARTICLE INFO

Article history:
Received 15 September 2019
Received in revised form 21 May 2020
Accepted 21 May 2020
Available online 23 May 2020

Keywords:
Glucose
Glucose dehydrogenase
NAD(P)
NAD
Biosensor
Biofuel cell

ABSTRACT

This review discusses the physical and chemical properties of nicotinamide redox cofactor dependent glucose dehydrogenase (NAD(P) dependent GDH) and its extensive application in biosensors and biofuel cells. GDHs from different organisms show diverse biochemical properties (e.g., activity and stability) and preferences towards cofactors, such as nicotinamide adenine dinucleotide (NAD^+) and nicotinamide adenine dinucleotide phosphate ($NADP^+$). The ($NAD(P)^+$) play important roles in biological electron transfer, however, there are some difficulties related to their application in devices that originate from their chemical properties and labile binding to the GDH enzyme. This review discusses the electrode modifications aimed at immobilising NAD^+ or $NADP^+$ cofactors and GDH at electrodes. Binding of the enzyme was achieved by appropriate protein engineering techniques, including polymerisation, hydrophobisation or hydrophilisation processes. Various enzyme-modified electrodes applied in biosensors, enzymatic fuel cells, and biobatteries are compared. Importantly, GDH can operate alone or as part of an enzymatic cascade, which often improves the functional parameters of the biofuel cell or simply allows use of cheaper fuels. Overall, this review explores how NAD(P)-dependent GDH has recently demonstrated high potential for use in various systems to generate electricity from biological sources for applications in implantable biomedical devices, wireless sensors, and portable electronic devices.

Contents

1. Introduction . . . 2
2. NAD(P)-dependent glucose 1-dehydrogenase: Structure and properties . . . 2
3. NAD(P)-dependent glucose 1-dehydrogenase for bioelectrodes and sensing . . . 4
   3.1. Nanostructured electrodes based on direct electrochemical oxidation of NAD(P)H . . . 4
   3.2. Various techniques to immobilise NAD^+ and GDH on solid substrates . . . 5
   3.3. Sensors using a mediator to oxidise NAD(P)H . . . 5
   3.4. Sensors using a second enzyme to oxidise NAD(P)H . . . 8
4. Biofuel cells with NAD(P)-GDH as the anode enzyme . . . 8
5. Perspectives . . . 12
   Declaration of Competing Interest . . . 14
   Acknowledgements . . . 15
   References . . . 15

* Corresponding author at: Faculty of Chemistry, University of Warsaw, Pasteura St 1, 02-093 Warsaw, Poland.
E-mail address: bilewicz@chem.uw.edu.pl (R. Bilewicz).

https://doi.org/10.1016/j.bioelechem.2020.107574
1567-5394/

1. Introduction

The oxidoreductase class of enzymes includes several subclasses, namely dehydrogenases, oxidases, reductases, peroxidases, oxygenases, catalases, and hydroxylases. All of these enzymes require cofactors, such as NAD, NADP, FMN, FAD, PQQ or CoQ, for their catalytic activities (NAD = nicotinamide adenine dinucleotide, NADP = nicotinamide adenine dinucleotide phosphate, FMN = flavin mononucleotide, FAD = flavin adenine dinucleotide, PQQ = pyrroloquinoline quinone, CoQ = Coenzyme Q). Many dehydrogenases used in bioelectrochemical research have been isolated from either gram-positive or gram-negative bacteria. They typically belong to the primary dehydrogenases located either on the outer surface of the cytoplasmic membranes (PQQ- or FAD-dependent dehydrogenases) or in the cytosol, as for the title NAD(P)-dependent dehydrogenases [1]. This means that besides PQQ also other cofactors with a similar structure exist: topaquinone (TPQ), tryptophyl tryptophanquinone (TTQ), lysine tyrosylquinone LTQ, and cysteine tryptophylquinone (CTQ) [2].

Bacterial quinoproteins represent one class of dehydrogenases, and depending on the enzyme, the natural electron acceptor is either a *c*-type cytochrome, a blue copper protein, or a membrane-bound ubiquinone molecule [3]. Most of these enzymes are closely associated with oxidative fermentation in various industries, where they are employed to catalyse an incomplete one-step oxidation and allow the transfer of an equivalent amount of corresponding oxidation product outside the cell [4]. All enzymatic dehydrogenase reactions are carried out by periplasmic oxidase systems, including those which oxidise alcohols or sugars [5,6]. Among these dehydrogenases, flavin-dependent enzymes are unique in the respect that they can participate in either one- or two-electron processes. In general, metalloenzymes catalyse only one-electron processes, whereas nicotinamide nucleotides are involved solely in two-electron processes, as their radical form is not sufficiently stable to be involved in the catalysis. The ($NADH/NAD^+$) or ($NADPH/NADP^+$) cofactors are relatively weakly bound to the protein structure and are easily released from the enzyme. This binding relationship is extremely important and leads to many of the challenges and specific properties involved with NAD(P)-dependent glucose dehydrogenases (GDH) that are discussed in this review.

2. NAD(P)-dependent glucose 1-dehydrogenase: Structure and properties

NAD(P)-dependent glucose 1-dehydrogenase, (NAD(P)-GDH; EC 1.1.1.47), has been isolated from both gram-positive and gram-negative bacteria, including *Bacillus amyloliquefaciens* [7], *Bacillus megaterium* [8,9], *Bacillus subtilis* [10], *Bacillus thuringiensis* [11], *Corynebacterium* sp. [12], *Gluconobacter oxydans* [13], *Lysinibacillus sphaericus* [14], as well as from mammalian sources, such as *Bos taurus* [15]. This group of enzymes shows similar activity with NAD^+ (EC 1.1.1.118) or $NADP^+$ (EC 1.1.1.119), and they were added to the enzyme catalogue in 1972 based on reports from Hu and Cline [16] and Avigad et al. [17]. Another group of GDH enzymes includes those which can only use NAD^+ as a cofactor (i.e., NAD^+-dependent glucose 1-dehydrogenases; EC 1.1.1.118), and a third group includes the enzymes depending only on $NADP^+$ as the cofactor (i.e., $NADP^+$-dependent glucose 1-dehydrogenase; EC 1.1.1.119). According to technical enzyme nomenclature, the second and third groups have been removed from the list of NAD(P)-dependent glucose 1-dehydrogenases, indicating that they should be treated independently. NAD(P)-dependent GDHs act only on the β-form of glucose (see Eq. (1)), catalysing the oxidation at the C1 position, therefore all of these enzymes are anomer-specific:

$$\beta\text{-D-glucose} + NAD(P)^+ \rightleftharpoons \text{D-glucono-1,5-lactone} + NAD(P)H + H^+ \quad (1)$$

GDH enzymes are intracellular proteins, and their isolation involves well-established, universally applied procedures, including optimisation of growing conditions and homogenisation. After purification using chromatographic techniques, GDHs from different organisms can be distinguished by their distinct biochemical properties (e.g., activity and stability) and preferences towards the cofactors (NAD^+ and $NADP^+$).

The species which produce NAD/NADP-dependent GDH and selected physical and chemical properties of the enzymes are collected in Table 1, complying with the rules of classifications of living organisms proposed by Ruggiero et al. [18].

Amino acid sequence alignment indicates that NAD(P)-dependent GDH from the *Bacillus* species (EC 1.1.1.47), belong to

Table 1
The taxonomy of species which produce NAD(P)-dependent glucose dehydrogenases and selected properties of these enzymes.

Organism [genus and species]	[superkingdom, kingdom]	pI	MW [kDa]	4D [mer]	pH opt.	Temp. opt. [°C]	Literature
Sulfolobus solfataricus	*Procariota; Archaea*	–	21	4x	6.5	–	[19,20,21]
Sulfolobus tokodaii	*Procariota; Archaea*	–	41	4x	–	75	[22]
Thermoplasma acidophilum	*Procariota; Archaea*	5.2	38	4x	10	70	[23,24]
Thermoproteus tenax	*Procariota; Archaea*	–	41	2x	–	–	[25]
Vulcanisaeta moutnovskia	*Procariota; Archaea*	–	38.6	–	–	–	[26]
Bacillus amyloliquefaciens	*Procariota; Eubacteria*	–	28	–	–	50	[7]
Bacillus megaterium	*Procariota; Eubacteria*	6.0	29	4x	–	25	[8,9,27,28]
Bacillus subtilis	*Procariota; Eubacteria*	4.7–4.8	31	4x	–	25	[29,30,31]
Bacillus turingiensis	*Procariota; Eubacteria*	–	25	2x	8.0	55	[32]
Corynobacterium sp.	*Procariota; Eubacteria*	4.05–4.4	48	1x	10.7	30–35	[12,33,34]
Lysinobacterium megaterium	*Procariota; Eubacteria*	–	30	4x	–	–	[35]
Lysinobacterium solfataricus	*Procariota; Eubacteria*	–	27.8	–	–	–	[36]
Lysinibacterium sphaericus	*Procariota; Eubacteria*	–	–	–	6.5	50	[14]
Oncorhynchus mykiss	*Eucariota; Animalia*	–	90	2x	10.5	–	[37]
Bos taurus	*Eucariota; Animalia*	–	59	4x	7.8–8.5	–	[15]
Homo sapiens	*Eucariota; Animalia*	–	89	2x	–	–	[38]
Mus musculus	*Eucariota; Animalia*	–	–	–	–	–	[38]
Rattus norvegicus	*Eucariota; Animalia*	–	98	–	–	–	[39]
Sus scrota	*Eucariota; Animalia*	7.1	58	4x	9.9	–	[40]

the extended superfamily of short chain dehydrogenases/reductases, due to their greater than 80% homology [9]. Their amino acid sequences can be found in various databases, including UniProtKB, Swiss-Prot, EMBL, PDB, OMIM, Pfam, or PROSITE [41]. These amino acid sequences can easily be translated *in silico* to the genome nucleotide sequences (and vice versa), and such data can be found in the TrEMBL supplement of the Swiss-Prot database. In the case of intracellular proteins, in order to discover large numbers of interesting enzymes, heterologous expression procedures (transferring the interesting gene into an efficient host cell) are required, since these processes provide a high level of amplification.

The NAD(P)-GDH gene from *Bacillus amyloliquefaciens* SB5 was transferred to and expressed in *E. coli* [7,42], and the same procedure was used regarding genes from *Bacillus megaterium* [27], *Bacillus subtilis* [43], *Sulfolobus solfataricus* [19], *Lysinibacterium sphaericus* [35], and *Sulfolobus tokodaii* [22]. The GDH from *Vulcanisaeta moutnovskia*, which belongs to the *Archaea* kingdom, was also characterised, and importantly, the detailed structure of this enzyme was determined. The protein peptide chain contains 351 amino acids with an overall molecular weight of 38.6 kDa and binds NAD or NADP, as well as Zn ions [26]. The molecular weight of NAD(P)-GDH varies from 28 kDa for the polypeptide chain isolated from *Bacillus megaterium* [44], to 84 kDa when isolated from *Thermoproteus tenax* [25]. Other glucose dehydrogenases have quaternary structure (subunits), and exist as a dimer in mammalian *Oncorhynchus mykiss* (2 × 90 kDa) [37] and *Bacillus thuringiensis* (2 × 28 kDa) [45], or as homotetramers in *Lysinibacillus megaterium* (4 × 30 kDa) [35] and *Sulfolobus solfataricus* (4 × 21 kDa) [46].

The isoelectric point of homogenic GDH varies between 4.05 and 4.4 for enzymes from different strains of *Corynebacterium* sp. [33], between 4.7 and 4.8 in the case of *Bacillus megaterium* [28], and is 4.9 for *Bacillus subtilis* [29], and 6.0 for *Bacillus megaterium* [28]. All of the enzymes mentioned above have activities that are highly specific for β-D-glucose. Specifically, for *Sulfolobus solfataricus* with an NADP co-substrate, the Michaelis-Menten constant, K_m, was found to be 0.17 mM, whereas, with NAD the value of K_m was 4.59 mM [20]. This enzyme's specificities for other substrates were also high, with a K_m of 0.44 mM for β-D-galactose [21] and 0.18 mM for D-xylose [21]. In the case of GDH enzymes from *Bacillus subtilis,* the K_m for 2-deoxy-β-D-glucose was 47.8 mM [29], 4.2 mM for 2-deoxy-D-glucose [30], and 35 mM for D-glucosamine [30]. Finally, for *Corynebacterium* sp. reacting with cellobiose, K_m = 11 mM [34], and with D-xylose, K_m = 125 mM [34].

Certain metal ions can influence the activity of NAD(P)-dependent GDH enzymes. For example, Li^+ ions (in the case of *Lysinibacillus sphaericus*) [35] and Ca^{2+} ions (in the case of *Sulfolobus solfataricus*) [47] enhance GDH enzymatic activity. In contrast, *Lysinbacterium megaterium* dehydrogenase activity is inhibited by Cu^{2+}, Cd^{2+}, Co^{2+}, Fe^{2+}, Fe^{3+}, Mn^{2+} or Zn^{2+} ions, and enhanced by EDTA [35]. In addition, the product of glucose oxidation (i.e., D-glucono-1,5-lactone), has demonstrated product inhibition for *Halobacterium salinarum* dehydrogenase [48]. Interestingly, ammonium sulphate, as well as NAD^+, NADH, $NADP^+$, NADPH, AMP, ADP, ATP, dipicolinic acid, Na_2SO_4, NaCl, and KCl can reactivate partially purified enzymes which have been inactivated by storage at 4 °C (AMP, ADP, and ATP refer to adenosine mono-, di-, and triphosphate, respectively) [49].

The optimal pH for GDH activity varies from 6.5 for *Lysinbacterium sphaericus* and *Sulfolobus solfataricus* [19,36], to 10.7 for *Corynebacterium* sp. [12]. Additionally, the ideal temperatures for individual enzymes range from 25 °C for *Bacillus licheniformis* [50] to 75 °C for *Sulfolobus tokodaii* [22]. These optimal temperatures for NAD(P)-dependent GDH enzymes depend on the organism from which they have been isolated. In general, psychrophiles, mesophiles, and thermophiles produce enzymes that act at similar temperatures (psychrozymes, mesozymes, and thermozymes, respectively) [51,52].

The pH stabilities of NAD(P)-dependent GDH enzymes are rather standard, according to the literature. After 30 min at 30 °C and at a pH between 3 and 11, the enzyme from *Bacillus thuringiensis* maintains over 70% of its initial activity, while NAD(P)-GDH isolated from *Corynebacterium* is still fully stable at pH between 6 and 8, and the *Bacillus subtilis* enzyme is extremely stable after incubation at pH from 4.5 to 10.5, retaining more than 80% of its original activity. In addition, some of the enzymes show considerable thermal stability. For example, after incubation for 30 min at temperatures of 25 to 80 °C, the enzyme from *Bacillus subtilis* maintains 20% of the maximum activity at its optimal temperature, 70 °C [31]. In the case of *Lysinbacterium sphaericus,* the GDH enzyme was stable for 1 week at 30 °C (pH 6.5), but it was completely inactivated after 30 min at 55 °C and lost 84% of its activity after 30 min of incubation at 65 °C in the presence of 2 M NaCl [35]. The *Thermoplasma acidophilum* enzyme showed high stability at 75 °C, with a half-life of 3 h in this incubation condition [23], while the enzyme from *Thermoproteus tenax* approached its half-life after only 10 min of incubation at 103 °C [25]. It was accepted for a long time that glycosylation is restricted to *Eukarya*, but since the beginning of the 21st century, it has been reported that this process can also occur in *Bacteria* and *Archaea* [53–56]. The mass of carbohydrates in glycoproteins can vary from below 1%, to more than 85% of the protein mass [57], and glycosylation processes can occur *via* N-glycosylation, O-glycosylation, or dolichol phosphate anchoring [58]. Specifically, the N-glycosylation in the case of *Archaea* and *Animalia* NAD(P)-dependent glucose dehydrogenases has been described by Yurist-Doutsch et al. [59] and Ruis-Canada et al. [60].

The different locations of the α-helical and the β-pleated sheet substructures in *Archaea*, *Eubacteria*, and *Animalia* should lead to different 3D structures of GDH enzymes and likely also different specificities and efficiencies. In the case of *Bacillus megaterium*, rapid inactivation of NAD-dependent GDH is observed following nitration of TYR-254 in the active tetramer. This process can be prevented in the presence of NAD, AMP, or ATP. After dissociation of the tetramer, TYR-160 can be modified by tetranitromethanol [61]. The crystal structure of NAD-GDH from *Bacillus megaterium* was determined to have an R-factor of 17.9% at 17 Å resolution, and it was found that the subunit structure shares the typical fold of short-chain dehydrogenases/reductases (SDRs) [62]. While a pair of basic residues is well-conserved, only ARG-39 was found around the adenine-ribose molecule, and the NAD cofactor is bound to the enzyme in its extended conformation at the carboxyl ends of the parallel β-sheets [63]. Its binding mode to the Rossmann fold is similar to that in other SDRs, with the adenine ring in the *anti*-conformation and the nicotinamide ring in the *syn*-conformation [64].

The NAD(P)-dependent GDH from the thermoacidophilic *Archaea*, *Thermoplasma acidophilum*, was crystalised, and it was found that its amino acid-sequence and protein structure were not homologous with the bacterial GDH enzymes [24]. The monomer consists of two domains, specifically a central nucleotide-binding domain (residues 187–300), flanked by the catalytic domain (residues 1–186, 301–352) [65]. The nucleotide-binding domain is comprised of a β-pleated sheet with six parallel strands (A to F), with a marked 100° left-handed twist within the sheet. It is similar to the nucleotide-binding domain of previously reported structures [66] and represents the core of the Rossmann fold structure, often called a βαβ fold. The β-pleated sheet is the most structurally conserved feature of the nucleotide-binding domain [66]. The sheet is flanked by four helices (ocB, aC, aE, ctF), which have different lengths from the flanking helices of other dehydrogenases. The central helix (residues 154–174) connects the nucleotide-binding domain to the amino-terminal region of the catalytic domain from the C-terminal end [67]. In the metagenome, the region for binding dinucleotides, such as $NAD(P)^+$, consists of

six parallel β-sheets with a relative strand order, β3- β2- β1- β4- β5- β6, flanked by α-helices [68]. Highly conserved sequence motifs for cofactor binding are present within the characteristic Rossmann-fold. In particular, the connecting loop between β-strand 1 and α-helix 1 is referred to as the ligand binding loop. The conserved amino acid residues in this loop region, along with the surrounding β-strand and α-helix, form the overall conserved sequence motif, V/IXGX1–2GXXGXXXG/A, for the Rossmann-fold, which is responsible for binding of NAD(P) or FAD [69].

3. NAD(P)-dependent glucose 1-dehydrogenase for bioelectrodes and sensing

The electrochemistry of the NAD(P)/NAD(P)H systems have been described in the chapter and review by Gorton and Domínguez [70,71] and Bartlett and Gorton [72]. The redox reaction involves two electrons and one proton, so it can be considered as a hydride transfer (Eq. (2)), with an E° of −0.315 V vs. NHE at pH 7 [70].

$$NAD(P)^+ + H^+ + 2e^- \rightleftharpoons NAD(P)H \quad (2)$$

The hydride transfer takes place at the C4 position of the nicotinamide ring, and the dehydrogenases show stereospecificity for the NAD(P)H. Specifically, some can transfer only the *R* hydrogen and some can only transfer the *S* hydrogen from the hydronicotinamide to their substrates. The same stereospecificity is observed in the reduction of NAD(P), i.e., introducing the hydrogen either to the *re*-face of the trigonal C4 or to the *si*-face (Fig. 1).

The reduced and oxidised forms of the nicotinamide cofactors are susceptible to decomposition in aqueous solution. The reduced forms of these cofactors are stable in base but labile in acid, and the oxidised forms are stable in acid but labile in base [73]. The optimal pH working conditions for NAD/NADH are in the range of 7–7.5, and for NADP/NADPH in the range of 8–8.5 [74]. The decomposition of NADPH additionally involves an intramolecular acid catalysis by the 2′-phosphate group [75]. In general, acid catalysts are most effective when their pK_a is approximately equal to the pH of the solution. The half-lives for the reduced dinucleotide cofactors (NADH and NADPH) are 27 and 13 h, respectively, in 0.1 M sodium phosphate at pH 7.

The basic redox reaction catalysed by NAD(P)-dependent dehydrogenase proceeds according to Eq. (1), where the nicotinamide cofactors are usually not covalently bound to the enzyme, so they can readily dissociate (K_D = 10^{-3}–10^{-5} M). The relatively low value of E° as compared with other biological redox reactions, in addition to other difficulties connected with the electrochemistry (i.e., high overpotential of NADH oxidation with common electrodes, fouling of the electrode by the products of direct oxidation, and the need for mediators) are all factors which have limited the interest in NAD(P)-dependent dehydrogenases relative to other enzymes. Moreover, the reduction of NAD^+ is also not a focus of interest due to the complexity of its reactions in combination with GDH.

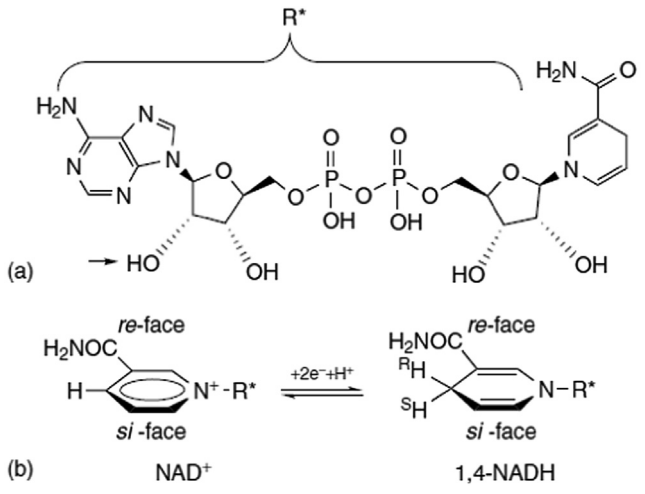

Fig. 1. (a) Enzymatically active 1,4-NADH (β-NAD reduced form), and (b) the stereospecific redox reaction between $NAD(P)^+$ and NAD(P)H. Reprinted with permission from Ref. [45].

The reports on NAD(P)-based bioelectrodes published up to 2006 are comprehensively reviewed in a book chapter by Bartlett and Gorton [72], therefore, these will not be discussed in detail in this review. Various approaches aimed at the fabrication of electrodes modified with NAD(P)-dependent GDH and electrochemical sensors based on this enzyme are considered there as well. Amperometric enzyme sensors based on direct and mediated electron transfer have also been described in a review by Schuhmann et al., however, the main focus was not specific to NAD(P)-dependent GDH-based sensors [76].

Amperometric biosensors employing NAD-dependent GDH as the catalyst have been used mainly for monitoring NADH production, and sometimes its consumption [76–79]. Most of the reactions catalysed by these dehydrogenases have E° values more positive than that of the NAD^+/NADH redox couple. The equilibrium of the reaction (Eq. (1)) only favours the production of NADH when the E° of this reaction is lower than that of the NAD^+/NADH redox couple, like for the oxidation of monosaccharides (glucose, galactose) or other aldehydes by their corresponding dehydrogenases. A GDH-based biosensor measuring the production of NADH requires that the NADH initially formed is instantaneously consumed by the mediator (or directly oxidised at the electrode surface), otherwise the reaction represented by Eq. (1) will reach equilibrium and further production of NADH will cease. The reduced mediator also must be re-oxidised rapidly to regenerate its active form. These factors mean that all three reactions (enzymatic, mediated, and electrochemical) need to occur harmoniously for successful catalysis. This reactivity is illustrated in Fig. 2 where, in the initial step, the electrons have to move against the thermodynamic driving force and couple with the mediator and the electrode, in order to realise a net thermodynamic driving force for NADH production.

Table 2 compiles selected important examples of sensing devices based on the application of NAD(P)-dependent GDH enzymes.

3.1. Nanostructured electrodes based on direct electrochemical oxidation of NAD(P)H

One significant challenge in terms of using an enzyme as an electrocatalyst, is to establish good electrical contact between the active site of the enzyme and the electrode surface. Achieving direct electron transfer (DET) between the enzyme and the electrode surface is difficult, because the active centre of the enzyme is usually located deep within the protein structure, so the distance between the electrode and the active site can be rather large. However, such transfer is possible when the active centre of the enzyme is located close to the outer surface of the protein, i.e., close to the surface of the electrode. One approach to obtain DET between the enzyme and the electrode surface is to employ various nanostructures, such as carbon paste [85], carbon nanotubes [92,95,99,101], quantum dots [117], inorganic clusters [118], or metal nanoparticles [120].

Nanomaterials are very efficient auxiliary materials to immobilise the enzyme due to their small size, excellent charge transport capabilities, and the ease of modification by attaching functional groups that enable covalent binding of the enzyme.

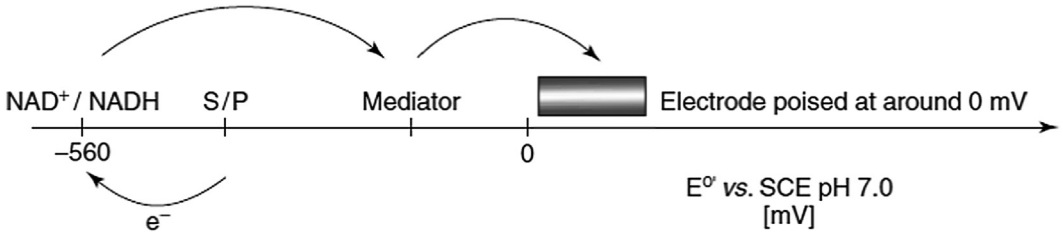

Fig. 2. Electron-transfer pathways in dehydrogenase-catalysed reactions coupled to electrodes via electrochemical reactions of the coenzymes. Electron fluxes represent oxidation of the substrate. Reprinted with permission from Ref. [72].

Nanostructures additionally allow for close contact between the enzyme active centre and the electrode substrate in a way that the enzyme activity can be maintained for a long time. Nanomaterials also significantly increase the surface area and capacitance of the electrode. Carbon nanotubes (CNTs) are a common example of nanostructures applied for facilitating DET. They have attractive structural, mechanical, and electronic properties, and they interact very well with the NAD^+ cofactor due to a strong π-π interaction between the adenine subunit of the NAD^+ molecule and the carbon nanotube material.

Carbon nanotubes are immobilised on the electrode surface (see Table 2) by placing the solution containing CNTs on the electrode and evaporating the solvent, or more effectively by using Nafion (Nf) or chitosan (CHIT) [92,95,110]. Chitosan is a polysaccharide biopolymer, which can form membranes, has high water permeability and good adhesion, and can be easily modified due to the presence of amine and hydroxyl functional groups. CHIT is especially convenient because it helps homogeneously disperse nanotubes, whereas preparing such homogeneous mixtures of CNTs in inorganic or organic solvents is often difficult or impossible. CNT-CHIT mixtures placed on the surface of glassy carbon electrodes (GCE) form stable CNT-CHIT films, which support NADH electrooxidation at a potential 0.3 V lower than for an unmodified GCE. CHIT can also be used to covalently immobilise GDH in CNT-CHIT films (see Table 2).

Recently, other research efforts have focused on using quantum dots to electrically connect such enzymes with conductive electrode supports. Ertek and co-workers [117] demonstrated that hybrid quantum dots (ZnS-CdS) adhered to the surface of a pencil graphite electrode (PGE) can promote DET with GDH. The electrode was also used for the photoelectrochemical determination of glucose concentrations in flow injection analysis (FIA).

Mahadevan and Fernando [118] presented an interesting approach to obtain DET after immobilizing GDH on an electrode. Specifically, they employed inorganic iron-sulphur (Fe-S) clusters (i.e., FeS, FeS_2, Fe_2S_3, and Fe_3S_4), which act as molecular wires. Voltammetric studies showed a significant improvement of the electron transport efficiency, as well as increased coverage of the electrode surface by the enzyme molecules. The authors explained such favourable electrode properties based on facilitated charge transport between NAD^+ and the electrode surface through the Fe-S clusters. In addition, the internal resistance of the enzyme electrode decreased due to the presence of the short FeS molecular wires and the ability of FeS to form single molecular anchors. Metal nanoparticles (NPs) are often used in sensing devices due to their high activity, which is associated with the presence of uncoordinated surface atoms in the nanostructures, and/or surface defects. Tamura and co-workers [120] observed direct electrochemical oxidation of NADH at extremely low overpotential (-0.075 V vs. Ag/AgCl) at pH 7.5 using a nanoporous gold (NPG) substrate, without any mediators. This result demonstrated an improvement in terms of overpotential of more than 0.6 V compared with a conventional gold electrode.

3.2. Various techniques to immobilise NAD^+ and GDH on solid substrates

Binding of an enzyme to an electrode can improve the stability of the enzyme-modified electrode system and may allow greater amounts of the enzyme molecules to be immobilised in an orientation that facilitates electron transfer. Two main advantages of using enzyme-modified electrodes are that (i) their working potential is close to the formal potential of the enzyme active centre, and (ii) it is relatively easy to achieve sensor miniaturisation. Any biosensor based on an NAD-dependent GDH that has the ambition of reaching the market must first resolve the issue of immobilizing sufficient amounts of NAD^+ within the biosensing device. The physical and chemical methods used to immobilise enzymes and NAD^+ on solid substrates include physical and/or chemical adsorption, cross-linking with conductive polymers, encapsulation in micelles, entrapment in a matrix, or immobilisation in a semi-permeable membrane. In general, physical immobilisation techniques do not have a significant effect on the structure of the enzyme. In contrast, covalent binding of a protein to the substrate may lead to modifications of the enzyme structure. Cross-linking is an approach often applied to immobilise enzymes, and during cross-linking with one, two-, or multi-functional cross-linking agents, multiple three-dimensional covalent bonds are created between the enzyme molecules. Despite the large variety of protein cross-linking agents, glutaraldehyde is the most commonly used due to its stability, low price, efficiency, and mild cross-linking conditions (see Table 2). The reactive aldehyde groups at the ends of this compound react with the free amino groups (ε-amino or N-terminal groups) in the enzyme to form Schiff base structures. The protein previously bound to the carrier may be also cross-linked, however, this should be considered as a complement to other immobilisation techniques. Gorski et al. prepared biosensors containing both GDH and NAD^+ using an approach based on the concept of molecular imprinting [95]. The novelty of this approach is that, although the dehydrogenase and cofactor are covalently attached to the polymer chains at the electrode surface, they still have sufficient freedom of movement to react with each other and provide reasonable current in the presence of glucose. In the system described, NAD^+ was covalently attached to chitosan polyaminosaccharide chains, and the bioaffinity interactions with GDH were enabled by cross-linking the CHIT with the modified glutaraldehyde. In addition, CNTs were deposited on the GCE, since they are known to increase the working surface area of the electrode [122,123]. Polyaminosaccharide chitosan chains can be considered as a convenient scaffold for covalent immobilisation of enzymes and redox cofactors, as well as for homogeneous dispersion of CNTs.

3.3. Sensors using a mediator to oxidise NAD(P)H

Due to the restricted lifetime of both NAD^+ and NADH, which are susceptible to decomposition in aqueous environments

Table 2
Examples of GDH-based glucose sensors.

Electrode composition	Applied voltage (V) vs. Ag/AgCl	Sensitivity (μA/(cm^2 mM)	LOD (μM)	Linear range (mM)	Solution	Year and Reference
GDH (from *Bacillus megaterium*), GR, MB	−0.050 V to 0 V vs. SCE	–	0.25	0.001–10	0.1 M phosphate buffer (pH 6.0), 1 mM NAD^+	1985 [80]
GDH (from *Bacillus megaterium*), MOB, NAD^+	0	–	–	0.005–2	0.1 M phosphate buffer (pH 6.0)	1986 [81]
GDH, BPT, GLD,	−0.2	–	–	0.003–0.5	0.1 M phosphate buffer (pH 7.0), 4 mM NAD^+	1991 [82]
GDH (from *Bacillus megaterium*), MOB, NAD^+, CP	0.1	–	–	0.1–20	0.25 M phosphate buffer (pH 7.0)	1991 [83]
GDH, NAD^+, NQS, PPy	–	–	–	0–20	0.1 M phosphate buffer (pH 7.0)	1991 [84]
GDH (from *Bacillus megaterium*), NAD^+, CP	–	–	–	0.1–0.9	0.1 M phosphate buffer (pH 7.5)	1991 [85]
GDH (from *Bacillus megaterium*), NAD^+, PMB, GLD, Nf	0.0 vs. SCE	–	–	0.01–10	0.1 M phosphate buffer (pH 7.7), 0.1 M KCl	1994 [86]
GDH (from *Bacillus megaterium*), TB, PEI or SPPT, GTN, NAD^+	0	25	–	up to 10	25 mM phosphate buffer (pH 7.0), 0.1 M KCl	1995 [87]
GDH (from *Bacillus megaterium*), osphendione, NAD^+, CP	0.15	–	–	up to 10	0.2 M phosphate buffer (pH 6.0)	1996 [88]
GDH (from *Bacillus megaterium*), NAD^+, PMB, PVAc	0.2 vs. SCE	–	–	0–50	0.1 M phosphate buffer (pH 7.0)	1996 [89]
GDH (from *Bacillus megaterium* M1286), $Ru(bpy)_3^{2+}$, EAQ or Nf, NAD^+	–	–	–	0.2–5	0.1 M phosphate buffer (pH 6.5)	1997 [90]
GDH, PTB	–	–	–	0.050–3	phosphate buffer (pH 6.8), 4 mM NAD^+	1998 [91]
GDH (from *Pseudomonas* sp.), GLD, CHIT, MWCNTs	0.4	80	3	0.005–0.3	phosphate buffer (pH 7.4), 0.10 mM NAD^+	2004 [92]
CNTP, 3,4-DHB	0.25	–	5	0.01–1	0.1 M phosphate buffer (pH 7.0), 0.3 μM GDH (from *Bacillus megaterium*), 1 mM NAD^+, 5 μM MAP, 5 μM Dp	2004 [93]
GDH (from *Thermoplasma acidophilus*), CNTP, Os redox polimer, Dp, NAD^+	0.2	13.4	10	up to 0.8	0.1 M phosphate buffer (pH 7.0)	2007 [94]
GDH (from *Pseudomonas* sp.), Nf, NAD^+, CHIT, MWCNTs	0.40	1.8	–	0.02–2	0.10 M phosphate buffer (pH 7.4)	2007 [95]
GDH, SWCNTs, NB, $NADP^+$, GLD	0.1	–	–	0–20	0.10 M phosphate buffer (pH 7.0)	2007 [96]
GDH (from *Pseudomonas* sp.), PNB, SWCNTs	0.05	–	5	0.1–8.5	0.1 M PBS (pH 8.5), 3 mM $NADP^+$	2008 [97]
GDH (from *T. acidophilum*, recombinant expressed *in E. coli*), AuNPs, THN, MWCNTs	0.2	7.8 μA/mM 18.5 μA/mM	5 (dark) 0.7 (light)	0.01–2.56 (dark) 0.001–3.25 (light)	0.1 M PBS (pH 7.0), 5 mM NADH	2008 [98]
GDH, SWCNTs, PPF	0.4	3.3	–	4.9–19	20 mM phosphate buffer (pH 7.4), 0.5 mM NAD^+	2008 [99]
GDH, PPF	0.6	0.320	–	2.5–26	20 mM phosphate buffer (pH 7.4), 0.5 mM NAD^+	2008 [100]
GDH (from *Aspergillus niger*), MWCNTs, NAD^+, GLD	0.30	0.474 μA/mM	4.81	0.010–0.300	0.10 M phosphate buffer (pH 7.0)	2010 [101]
GDH (from *Bacillus* sp.), MOB, SPCE, NAD^+, GLD	0.05	0.051 μA/mM	50	0.075–30	0.2 M PBS (pH 7.0)	2010 [102]
GDH (from *Bacillus* sp.), NB, SWCNTs-COOH, NAD^+, CA, GLD	0.0	14	0.3	0.100–1.7	0.1 M PBS (pH 6.0), 10 mM NAD^+	2011 [103]
GDH (from *Pseudomonas* sp.), SWCNTs, MG, $Bmim^+Gly^-$, $Bmim^+NAD^-$, GLD	0.20	–	–	0.020–3.8	0.10 M phosphate buffer (pH 7.0)	2011 [104]
GDH (from *Pseudomonas* sp.), Ru $(bpy)_3^{2+}$, MPSG, PEG-400, Resy	1.3	–	0.5	0.025–2	0.1 M phosphate buffer (pH 7.5), 2.5 mM NAD^+	2011 [105]
GDH (from *Bacillus* sp.), SWCNTs-PPS	0.0	96.5	0.3	0.050–0.700	0.1 M PBS (pH 7.0), 10 mM NAD^+	2012 [106]
GDH (from *Thermoplasma acidophilum*, recombinant expressed in *E coli*), CHIT, BMIMPF6 IL	0.25	5.3 (μA/mM)	9	0.020–1	PBS (pH 7.4), 1 mM NADH	2012 [107]
GDH, SWCNTs, PPF, PT	0.2	5.1	120	4.9–19.0	20 mM phosphate buffer (pH 7.4), 0.5 mM NAD^+	2012 [108]
GDH, RGO, FePhenTPy, NAD^+, Nf	0.55	–	6.7	0.017–0.330	0.1 M PBS (pH 7.4)	2013 [109]
GDH (from *E. coli*), MWCNTs, Nf,	0.5	–	4	0.050–0.800	0.1 M PBS (pH 7.4), 1 mM NAD^+	2013 [110]
GDH (from *Pseudomonas* spp.), ZIFs, MG	0	–	–	0.1–2	0.10 M phosphate-buffered (pH 7.0), 5 mM NAD^+	2013 [111]
GDH (from *Pseudomonas* sp.), SAF, MWCNTs-NH_2, PAMAM-Den	–	–	0.5	0–5	PBS (pH 6.0), 10 mM NAD^+	2013 [112]
GDH, RGO, CdS QDs, PNB, PBA	−0.02	–	–	up to 0.25	0.1 M PBS (pH 7.0), 10 mM NAD^+	2014 [113]

Table 2 (*continued*)

Electrode composition	Applied voltage (V) vs. Ag/AgCl	Sensitivity (μA/(cm^2 mM)	LOD (μM)	Linear range (mM)	Solution	Year and Reference
GDH, FePhenTPy, NAD^+	0.350	0.57 μA/mM	14.81 mg/dL	30–500 mg/dL	0.1 M PBS (pH 7.4)	2015 [114]
GDH (from *Pseudomonas* sp.), PHT, PAMAM-Den	0.3 after irradiation, 0.3	0.76 μA/mM 1.90 μA/mM	3 1.5	0.01–1 0.005–1	0.1 M PBS (pH 7.0), 0.1 M KCl, 10 mM NAD^+	2015 [115]
GDH (from *Pseudomonas* sp.), [Ni(phendion)(phen)]Cl_2, MWCNTs	0.1	–	–	0–0.06	PBS (pH 7.0), 10 mM NAD^+	2015 [116]
GDH (from *Pseudomonas* sp.), ZnS–CdS QDs, MAA	0.8	–	50	0.2–8.0	0.1 M phosphate buffer (pH 7.0), 1.0 M KCl, 10 mM NAD^+	2016 [117]
GDH (from *Bacillus* sp.), FeS, GLD, NAD^+	0.50	25.21	770	0.1–100	0.1 M Tris-HCl buffer (pH 8.0)	2018 [118]
GDH (from *Bacillus* sp.), FeS_2, GLD, NAD^+	0.50	15.62	1220	0.1–100	0.1 M Tris-HCl buffer (pH 8.0)	2018 [118]
GDH (from *Bacillus* sp.), Fe_2S_3, GLD, NAD^+	0.50	15.01	2950	0.1–100	0.1 M Tris-HCl buffer (pH 8.0)	2018 [118]
GDH (from *Bacillus* sp.), Fe_3S_4, GLD, NAD^+	0.50	23.79	1457	0.1–100	0.1 M Tris-HCl buffer (pH 8.0)	2018 [118]
GDH (from *Bacillus* sp.), Cys, APB, PQQ, GLD, NAD^+	0.50	12.92	3720	0.1–100	0.1 M Tris-HCl buffer (pH 8.0)	2018 [118]
GDH (from *Pseudomonas* sp.), PMB, PAMAM-Den, GLD	0.2	5.0	4.0	0.010–1	0.1 M PBS (pH 7.0), 10 mM NAD^+	2018 [119]
GDH (from *Bacillus megaterium* (BmGDH-IV)), NPG	−0.15	1.2 μA/mM	–	0.01–0.4	phosphate buffer (pH 6.0), 0.57 μM BmGDH-IV (wild-type), 0.1 mM NADH, 300 mM NaCl	2019 [120]
GDH (from *Bacillus megaterium* (BmGDH-IV)), NPG	−0.15	0.12 μA/mM	–	0.4–16	phosphate buffer (pH 6.0), 0.57 μM BmGDH-IV (mutant G259A), 0.1 mM NADH, 300 mM NaCl	2019 [120]
GDH (from *Pseudomonas* sp.), Dp	0.0	–	200	0.1–30	PBS (pH 7.4), 10 mM $Os(bpy)_2Cl_2$, 2.0 mM NAD^+	2019 [121]

Abbreviations: single walled carbon nanotubes (SWCNTs), multi-walled carbon nanotubes (MWCNTs), carbon nanotubes (CNTs), COOH-functionalized SWCNTs (SWCNTs-COOH), amine functionalized multiwall carbon nanotubes (MWCNTs-NH_2), graphite rods (GR), meldola blue (MOB), toluidine blue (TB), chitosan (CHIT), polyethyleneimine (PEI), poly[N,N'-(sulpho-p-phenylene) terephthalamide] (SPPT), gentamicin (GTN), tris(2,2′-bipyridyl)ruthenium(II) ($Ru(bpy)_3^{2-}$), Eastman AQ (EAQ), Nafion (Nf), poly-toluidine blue (PTB), chitosan (CHIT), glutaraldehyde (GLD), 3,4-dihydroxybenzaldehyde (3,4-DHB), diaphorase (Dp), carbon nanotube paste (CNTP), poly(1-vinylimidazole)$_{12}$-[osmium(4,4′-dimethyl-2,2′-dipyridyl)$_2Cl_2$]$^{2+/+}$ (Os redox polymer), nile blue (NB), poly-nile blue (PNB), thionine (THN), gold nanoparticles (AuNPs), plasma-polymerized thin film (PPF), screen-printed carbon electrode (SPCE), cellulose acetate (CA), methylene green (MG), 1-butyl-3-methylimidazolium glycine ($Bmim^+Gly^-$), tris(2,2′-bipyridyl) ruthenium(II) chloride hexahydrate ($Ru(bpy)_3^{2+}$), mesoporous silica sol–gel (MPSG), Resydrol (Resy), polyethylene glycol 400 (PEG-400), poly(phenosafranin)-functionalized single-walled carbon nanotubes (SWCNTs-PPS), 1-butyl-3-methylimidazolium hexafluorophosphate ionic liquid (BMIMPF6) IL, phenothiazine (PT), plasma-polymerized thin film (PPF), reduces graphene oxide (RGO), 5-[2,5-di(thiophen-2-yl)-1H-pyrrol-1-yl]-1,10-phenanthroline iron(III) chloride (FePhenTPy), zeolitic imidazolate frameworks (ZIFs), methylene green (MG), safranin (SAF), amine-derivative multiwalled carbon nanotubes (MWCNTs-NH_2), carboxylated polyamidoamine dendrimer (PAMAM-Den), CdS quantum dots (CdS QDs), 1-pyrene butyric acid (PBA), 5-(2,5 di(thiophen-2-yl)-1H–pyrrol-1-yl)-1,10-phenanthroline iron(III) chloride (Fe-PhenTPy), hematoxylin film (PHT), 1,10-phenanthroline-5,6-dione and 5-amino-1,10-phenanthrolin ([Ni(phendion)(phen)]Cl_2), hybrid ZnS–CdS quantum dots (ZnS–CdS QDs), mercapto acetic acid (MAA), iron (II) sulphide (FeS), iron disulphide (FeS_2), iron(III) sulphide (Fe_2S_3), Greigite (Fe_3S_4), pyrroloquinoline quinone (PQQ), 3-aminophenyl boronic acid monohydrate (APB), cystamine (Cys), methylene blue (MB), poly methylene blue (PMB), nanoporous gold (NPG), bis(2,2-bipyridyl)dichloroosmium(II) [$Os(bpy)2Cl_2$], poly(vinylacetate)-poly(ethylene)-copolymer (PVAc), poly(pyrrole) (PPy), 3-naphthoquinonesulphonate (NQS), carbon paste (CP), Os(4,4′-dimethyl, 2,2′-bipyridine)$_2$(l,10-phenanthroline-5,6-dione (osphendione), bls(benzophenoxazinyl) derivative of benzene-1,4-dicarboxamide (BPT), p-methylamino-phenolsulphate (MAP).

[124,125], co-immobilisation of NAD^+ onto composite electrodes [126–129] or in electropolymerised layers [130] together with the enzyme and a mediator seems to be the preferred approach (see Table 2). In these systems, it is crucial that the mediated reaction is very fast, therefore, finding optimal mediators is an active area of research [131]. In general, a mediator should have a low formal potential to effectively decrease the overpotential of coenzyme oxidation, and good adsorption on various nanomaterials so that it can remain attached to nanostructured electrodes. Among the redox mediators used for electrocatalytic oxidation of NADH, the most common are azine dyes, such as methylene blue (MB) [80,86,89,119], toluidine blue (TB) [87,91], meldola blue (MOB) [81,83,102], nile blue (NB) [96,97,103], and methylene green (MG) [104,111] (see Table 2). Monomeric MB has favourable electrocatalytic properties for NADH electrooxidation, including a low electrode potential, and can be easily polymerised on an electrode. Importantly, the polymerised methylene blue (PMB) layers are smooth and electroactive [86,89,119].

An elegant approach outlined by Willner et al. involved covalent coupling of an enzyme-active NAD^+ analogue with a mediator (PQQ), which, in turn, was tethered to a gold electrode [132–136]. Biosensors responsive to substrates of NAD^+-dependent GDH were fabricated based on methacrylate-based redox polymers bearing covalently-bound redox dyes, such as TB or NB [137]. Other electron mediators often used in glucose sensors are organometallic complexes of ruthenium [90,105], osmium [88,94,121], iron [109,114], or nickel [116]. In general, electronic mediation by larger ruthenium complexes is a slow process compared with other mediators, and Os complexes are usually preferred among these organometallic mediators because they operate rapidly and are relatively more stable and more resistant to interferences than others. Modification of Os complexes allows for fine-tuning the redox potential as needed, and many Os complexes have been proposed as convenient, biocompatible mediators.

The development of a sensor that can work continuously in a flow system would provide the opportunity to automate the work of a sensor in an industrial environment. Hart and co-workers [102] developed a biosensor for measuring blood glucose based on an MOB-modified carbon electrode. The sensor was coated with a cellulose acetate layer, which acts as a permselective membrane, and its response was linear in the range of 0.075–30 mM glucose. These prototypical biosensors have been shown to be stable for at least 240 days, and the devices allow for low-cost, high-throughput analysis of clinically important serum analytes without any prior treatment. Another electrochemical detection system for *in vivo* monitoring of glucose in the cerebral system [111] is shown in Fig. 3.

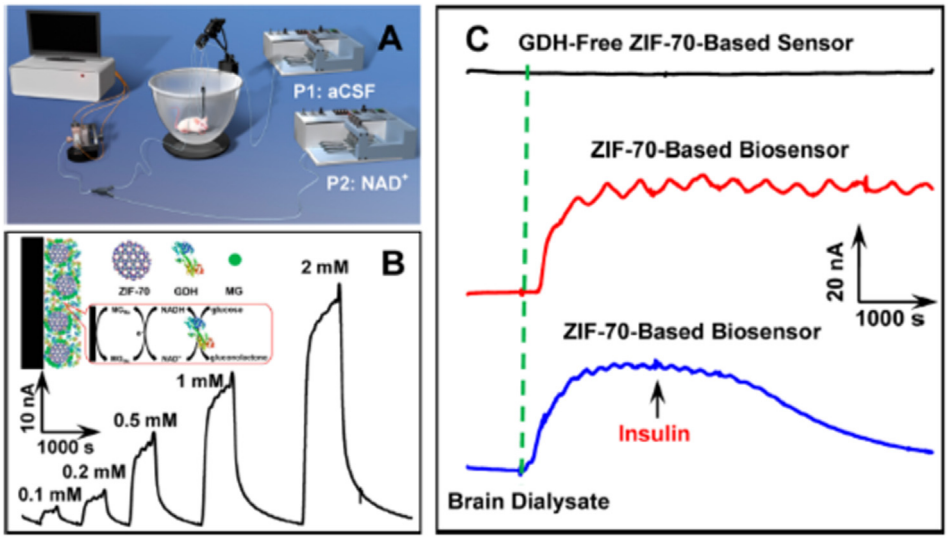

Fig. 3. (A) Schematic illustration of the online electrochemical detection system for *in vivo* monitoring of glucose in the cerebral system. (B) Online current–time response for glucose standards (with concentrations indicated in the figure) recorded using the online detecting system with a ZIF-70-based biosensor as the detector. Inset: schematic illustration of the ZIF-70-based biosensor. (C) Online current–time response recorded for the brain microdialysates of guinea pig on the online detecting systems. The brain microdialysate was continuously sampled from pump 1 (P1) and mixed online with pure NAD^+ solution (5.0 mM) from pump 2 (P2). Reprinted with permission from Ref. [111].

3.4. Sensors using a second enzyme to oxidise NAD(P)H

The diaphorase (Dp; EC 1.6.99.1) enzyme shows very fast reactivity with NADH, as well as oxygen insensitivity and excellent thermal stability up to 70 °C. Therefore, this enzyme has been incorporated into several biosensors based on GDH [93,94,121]. The application of Dp together with GDH requires the use of a mediator, which may cause additional construction issues, despite the high bimolecular rate constants between Dp and organometallic mediators (>10^8 $M^{-1}s^{-1}$). Antiochia and Gorton [94] prepared an amperometric biosensor via simultaneous immobilisation of GDH, Dp, and NAD^+ on a carbon nanotube paste (CNTP) electrode modified with a functionalised osmium polymer. The osmium-based mediator effectively transferred electrons between the immobilised Dp and the CNTP electrode, showing overall high electrocatalytic activity towards NADH oxidation at potentials around + 0.2 V vs. Ag/AgCl. The amperometric biosensor was applied for monitoring glucose concentrations in alcoholic beverages (i.e., sweet wine samples), and it was reported to have a good linear working range, sufficiently low detection limit (10 μmol/L), good reproducibility, and high stability. Due to the nature of the sensor, it was insensitive to the concentration of molecular oxygen, so deoxygenation of the samples was not necessary. The results of amperometric determination of glucose levels in sweet wine samples were consistent with those obtained by standard spectrophotometric methods. Recently, application of the two enzyme approach (with Dp and another non-GDH enzyme) to screen-printed carbon electrodes modified with graphene oxide was proposed for the design of a reagent-free NAD^+ dependent biosensor array, which is useful for multianalyte, simultaneous detection of L-lactate, D-lactate, ethanol, and formate [138].

4. Biofuel cells with NAD(P)-GDH as the anode enzyme

NAD(P)-dependent GDH enzymes have often been used to construct bioanodes in biofuel cells (BFC) because, unlike for glucose oxidase, GDH is not reduced during the oxidation of the molecular oxygen substrate, and the maximum activity is achieved at physiological conditions, close to pH 7 [139,140]. Therefore, GDH initially used in glucose biosensors was quickly adapted for the construction of bioanodes used in fuel cells [141]. However, its labile active centre caused some difficulty, in that it is necessary to either dissolve the NAD^+ in solution or immobilise it on the electrode to allow for the proper functioning of the enzyme. The use of NAD^+-dependent GDH is advantageous because glucose oxidation takes place at a much lower overpotential than that of PQQ-dependent GDH, for example [140]. This makes NAD-GDH more attractive for electrochemical applications, and particularly for bioenergy generation. Nishizawa and co-workers [142] described an NAD^+-dependent GDH-based biobattery in which the anode is covered with a double membrane layer using diaphorase in the inner layer and GDH in the external layer. The Dp membrane was formed from a newly synthesised polymer, based on 2-methyl-1,4-naphthoquinone (vitamin K3; VK3), which often serves as a mediator, and ketjenblack was used as the conductive support. The polymer derived from 2-methyl-1,4-naphthoquinone exhibited reversible redox activity near that of free VK3 (0.25 V vs. Ag/AgCl in saturated KCl) and served as a Dp electron mediator for the electrocatalytic oxidation of NADH to NAD^+. The addition of a conductive carrier, ketjenblack (KB), to the Dp/VK3 film significantly increased the production of NAD^+, and thus the activity of the outer membrane GDHs. The external GDH membrane oxidised glucose continuously using the NAD^+ generated at the inner Dp layer. Rather than an enzymatic electrode, this biofuel cell employed a Pt electrode coated with polydimethylsiloxane (PDMS) as the cathode. The open circuit voltage (OCV) was 0.62 V, and its maximum power density was 12.8 μW/cm^2 at approximately 0.35 V, in an air saturated phosphate buffered saline (PBS, pH 7.0) solution containing 0.5 mM NADH and 10 mM glucose at 37 °C. After 5 days of operation, its power dropped by about 8 μW/cm^2, but after this time, the cell power density was maintained for more than 2 weeks. The two-layer structure allows the use of various NAD^+-dependent enzymes, not only GDH, and the fact that VK3 is chemically harmless is another attractive aspect in terms of potential implant applications.

A fuel cell that can be structured without a membrane simplifies the construction and lowers the overall cost of the cell. Mao and co-workers [143] described one of the first biofuel cells without a membrane. It contained an anode coated with single-walled

carbon nanotubes (SWCNTs) and GDH, with NAD^+ as a freely dissolved cofactor in the buffer solution. The cathode was similarly coated with carbon nanotubes modified with laccase as the biocatalyst for O_2 reduction, and methylene blue adsorbed on SWCNTs was used to support the oxidation of NADH. The OCV of this system was 0.80 V, and the power density was 9.5 $\mu W/cm^2$ at 0.52 V. When the biofuel cell operated continuously for one week in aerated 0.10 M phosphate buffer containing 10 mM NAD^+ and 30 mM glucose at pH 6.0, it lost approximately 20% of its initial power in the first 24 h, then about 5% daily. SWCNTs provide a large conductive surface area and are still the most often employed carbon-based nanostructuring material used to improve the voltage and current of enzymatic BFCs. Willner and co-workers [96] employed SWCNTs with covalently bound NAD^+ or $NADP^+$ to construct the enzyme electrodes. In this case, the SWCNTs were further functionalised with nile blue (instead of MB), and the $NADP^+$ and NAD^+ cofactors were connected to that NB through a phenyl boronic acid ligand. Similarly, GDH and $NADP^+$ were cross-linked to the electrode with glutaraldehyde. Biocompatible polymers are suitable materials for the construction of bioelectrodes because they provide a protective layer for the enzymes at the electrode interface, while allowing them to fully maintain their activity. Glutaraldehyde is often used for such cross-linking since, as described previously (*vide infra*), it generates a stable enzyme coating. Electrocatalytic glucose oxidation by this cell at pH 7.0 occurred at a potential of −0.15 V vs. Ag/AgCl, and the linear dependence of current on the glucose concentration was observed in the range of 0 to 20 mM. The biocathode was modified with SWCNTs cross-linked with bilirubin oxidase (BOD; EC 1.3.3.5) using glutaraldehyde. The bioelectrodes were ultimately assembled in the biofuel cell, which exhibited an OCV of 0.7 V and a maximum power density of 23 $\mu W/cm^2$ at about 0.3 V. Ohsaka and co-workers [103] also immobilised GDH with NB covalently mounted on the surface of a GCE which had been modified with SWCNTs chemically functionalised with carboxylic acid groups. The biocathode was prepared by applying SWCNTs modified with MG and laccase (EC 1.10.3.2) in a bovine serum albumin (BSA) matrix onto a GCE. The OCV of this fuel cell in 0.1 M PBS (pH 6.0) solution containing 10 mM NAD^+ and 40 mM glucose under O_2 atmosphere was 0.85 V, with a maximum power density reaching 32.0 $\mu W/cm^2$ at 0.35 V. Korani and Salimi [144] used a glassy carbon electrode modified with amine functionalised multi-walled carbon nanotubes (MWCNTs-NH_2), GDH, and NB as the anode, and a carboxylated polyamidoamine dendrimer (PAMAM-Den) was employed as a multifunctional linker. The enzyme was efficiently immobilised on DNA-modified MWCNTs at the cathode due to their enhanced negative charge density, which was proposed as a novel electrochemical platform for oriented immobilisation of BOD. In this biofuel cell, the OCV was 0.660 V and the maximum power density was 45 $\mu W/cm^2$ at 0.428 V in an O_2 saturated buffer containing 50 mM glucose. The stability of the biofuel cell was tested in a continuous mode of operation at maximum power, and it was observed that the biofuel cell retained over 85% of its power and potential efficiency after 24 h.

The search for new compounds that can support the oxidation of NADH is an important issue in the development of biofuel cells based on NAD(P)-dependent GDH, when meldola blue is applied instead of nile blue as the electrocatalyst for NADH oxidation [145]. Dong and co-workers [146] fabricated a miniature BFC using a carbon fibre anode covered with MOB-modified single-walled carbon nanohorns (SWNHs or SWCNHs) to oxidise NADH in the immobilised GDH. Carbon fibre microelectrodes with SWNHs and immobilised BOD were used to reduce O_2 to H_2O at the cathode. The maximum output power of this cell was 140 $\mu W/cm^2$ at 0.51 V using various types of non-alcoholic beverages as sources of biofuel. In another report, Dong and co-workers [147] employed ionic liquid-functionalised carbon nanocomposites (CNTs-IL) coated with NAD^+-dependent GDH for the oxidation of glucose, and employed BOD for O_2 reduction. The biofuel cell containing only 30 μL of 0.1 M PBS solution (pH 7) with 10 mM NAD^+ and 30 mM glucose had an OCV of 0.56 V, and a maximum power density of 13.5 $\mu W/cm^2$ was obtained at 0.33 V. Power could be continuously generated with this BFC by adding 30 μL aliquots of fresh fuel, and a power loss of only 7% was observed when the cell was stored at 4 °C for one week. The device was also tested in beverages containing natural glucose fuel (e.g., Nescafe, Maidong vitamin water, fresh watermelon juice, and Minute Maid grape juice). Minteer and co-workers [148] used a naphthoquinone redox polymer for both immobilisation of GDH and oxidation of the enzymatically produced NADH. The main advantages of using this redox polymer are its excellent ability to immobilise NAD-dependent enzymes in a three-dimensional network, and its low cost compared with PQQ-based systems and other analogous polymer agents. The biocathode for the cell was prepared using MWCNTs with anthracene groups, which promote proper orientation of the type 1 Cu centre of laccase and allow direct electron transfer. The glucose/O_2 biofuel cell had an OCV of 0.766 V and maximum current and power densities of 505.7 $\mu A/cm^2$ and 123.2 $\mu W/cm^2$, respectively. The anode and cathode chambers were separated by a Nafion membrane to prevent cross-over and competitive oxidation of NADH at the biocathode. In another study by these authors [149], the benzylpropylviologen-linear-poly(ethyleneimine) redox polymer (BVP-LPEI; N-benzyl-N'-propyl-4,4′-bipyridinium) was used in combination with NAD^+-dependent GDH and Dp, and it was found to facilitate the inter-conversion of NAD^+/NADH on the surface of the carbon electrode. Anthracene-modified MWCNTs and laccase were employed at the cathode of this cell, which had an OCV of 1.1 V and a maximum current density and power density of 41.4 $\mu A/cm^2$ and 31.3 $\mu W/cm^2$, respectively. In order to operate, the anolyte and catholyte had to be separated by a Nafion proton exchange membrane.

Mao and co-workers [150] constructed a glucose/O_2-based biofuel cell using an anode employing poly(brilliant cresol blue) (BCB) adsorbed on SWCNTs and GDH to promote NADH oxidation and a BOD-modified cathode. Compared with a biofuel cell based on GDH with poly methylene blue (PMB) [143] as the electrocatalyst for NADH oxidation, the application of BCB resulted in a decrease in the overpotential at the bioanode. The biocathode was prepared by cross-linking BOD with glutaraldehyde on the SWCNT-coated electrode. In O_2-saturated 0.10 M phosphate buffer solution containing 10 mM NAD^+ and 40 mM glucose, the power density of the cell reached 53.9 $\mu W/cm^2$ at 0.50 V. This system was also tested in O_2-saturated serum containing 10 mM NAD^+. In this case, the OCV of the biofuel cell was 0.63 V, and the power density was 5 $\mu W/cm^2$ at 0.45 V, significantly lower than those of the BFC in the phosphate buffer, due to the lower concentration of glucose and the presence of additional chemical species in the serum, such as urate and ascorbic acid. Mao and co-workers [151] more recently described a glucose/O_2 BFC with high tolerance for the physiological level of ascorbic acid (AA) achieved by immobilizing ascorbate oxidase (AAox; EC 1.10.3.3) at the electrodes and employing GDH and BOD as the biocatalysts. Carbon microelectrodes coated with SWCNTs and PMB were used to catalyse the oxidation of NADH and facilitate reduction of O_2 by BOD. The maximum power density and OCV for this call were 52 $\mu W/cm^2$ and 0.60 V, respectively. Interestingly, these values did not change in the presence of AA in the solution. In aerated human serum containing 10 mM NAD^+, the maximum power density and OCV were 35 $\mu W/cm^2$ and 0.39 V, respectively. This demonstrated high tolerance in the presence of AA allows for use of the proposed devices under biological conditions.

Transition metal complexes have also been used to support NADH oxidation. For example, Hadadzadeh and co-workers [116]

used a nickel complex, [Ni(phendion)(phen)]Cl_2 (phendion = 1,10-phenanthrolin-5,6-dione; phen = 5-amino-1,10-phenanthrolin), which was covalently attached to a GCE with carboxyl-functionalised, multi-walled carbon nanotubes (MWCNT-COOH). GDH was then immobilised on the electrode via cross-linking, and the system was used for glucose oxidation. A GCE with MWCNTs and gold nanoparticles (AuNPs) was used for the immobilisation of the BOD enzyme. The OCV and the maximum current density are 520 mV and 0.233 mA/cm^2, respectively, in a stirring, O_2-saturated PBS solution containing 10 mM NAD^+ and 100 mM glucose. Nishizawa and co-workers [152] proposed a glucose/O_2 flow cell system, where the bioanode was carbon black (i.e., ketjenblack (KB) containing vitamin K3-modified poly-L-lysine (PLL-VK3). It served as an electron transfer mediator during the catalytic oxidation of NADH by diaphorase. Both PLL-VK3 and Dp were immobilised on the electrode and then coated with NAD^+-GDH, and Pt coated with PDMS was used as the cathode. The OCV of the cell was 0.55 V and its maximum power density was 32 μW/cm^2 at 0.29 V when pH 7.0 buffer containing 5.0 mM glucose and 1.0 mM NAD^+ was used at a flow rate of 1.0 mL/min. Immobilizing NAD^+ on the electrode has always been considered as a convenient approach, since it does not require the addition of NAD^+ to the solution, thereby also significantly reducing the cost of bioanode preparation. Another BFC, wherein ketjenblack (KB) with physically adsorbed BOD was used as the cathode, could operate without any mediators and showed a maximum power density of 52 μW/cm^2 at 0.3 V, which was sufficient to power the latest models of medical sensors [153]. Ketjenblack (KB) electrodes with immobilised NAD^+ have been proposed for many other NAD^+-dependent dehydrogenase enzyme systems, such as alcohol dehydrogenase and glutamate dehydrogenase, as well as for multi-fuel or multi-stage oxidation devices [154–156].

In general, a minimum of 100 mW of power is required to power portable devices. To accomplish this goal, significant research efforts have focused on improving the structure of electrodes and electrolytes, the manner of immobilizing enzymes, and the application of an appropriate combination of multiple enzymes on the surface of an electrode. A simpler method is to use serial or parallel connected biofuel cells. A common approach is to use the Layer-by-Layer (LbL) method of film deposition. In this way, several three-dimensional (3-D) systems were designed in order to increase the performance of electrodes intended for use in biofuel cells. Dong and co-workers [157] described a single-chamber glucose/O_2 biofuel cell based on the electrostatic self-assembly technique, LbL, to form a 3-D, ordered, macroporous gold electrode (3DOM). These gold electrodes were functionalised with AuNPs and an enzyme, typically GDH or laccase. Anodes comprised of gold electrodes modified with AuNPs/GDH multilayers, and gold cathode electrodes modified with AuNPs/laccase multilayers show excellent bioelectrocatalytic activity with respect to glucose and oxygen, respectively. The developed procedure led to increased immobilisation of the enzymes and improved overall biofuel cell parameters. The OCV for the cell described was 0.32 V and the maximum power density was 178 μW/cm^2 at 0.226 V, which is 16 times higher than a BFC with a flat electrode working under the same conditions. The proposed methods of 3DOM electrode assembly and the LbL technique are simple and useful tools to increase the output power of miniaturised biofuel cells. In another report, Dong and co-workers [158] increased the power of the biofuel cell to 329 μW/cm^2 at 0.470 V in air-saturated 0.1 M PBS (pH 6.0) containing 10 mM NADH and 30 mM glucose. Specifically, the LbL technique was applied for the deposition of MWCNTs, laccase and poly-L-lysine (PLL) on the cathode, and MWCNTs, thionine, gold nanoparticles, and GDH on the anode to generate a cell with a reported OCV of 0.7 V.

Toma and co-workers [159] improved upon the performance of the biobattery by incorporating the activity of three enzymatic reactions using GDH, Dp, and BOD. Instead of a glassy carbon electrode (GCE), a thin, elastic Pt electrode was used as a substrate on which the enzymes, coenzyme, and mediators were immobilised via the LbL method. The maximum current and power densities of the constructed biobattery were 257 μA/cm^2 and 86 μW/cm^2, respectively, in 5 mM glucose solution. The unique construction of this biofuel cell allowed for reduced internal resistance by shortening the distance between the anode and the cathode. Additionally, the oxygen supply to the biocathode was increased using a very porous cotton diaphragm mesh, and as a result, the biobattery with enhanced air breathing capability showed maximum current and power densities of 451 μA/cm^2 and 162 μW/cm^2, respectively. The increased oxygen supply to the cathode revealed a proportional relationship between the increase in power density and the rise in oxygen concentration. During continuous operation for 210 min, the biobattery demonstrated highly stable energy production, indicated by only a 3.3% drop over the entire working period. Kano and co-workers [160] prepared a glucose/O_2 biofuel cell composed of a carbon fibre (CF) anode coated with successive layers of PLL, GDH, Dp, NADH, VK3, and polyacrylic acid sodium salt (PAANa). The CF cathode was coated by deposition of $K_3[Fe(CN)_6]$, PLL, and BOD. In the presence of air-saturated 0.4 mg glucose/1.0 M PBS (pH 7.0) solution, the biofuel cell reached a maximum power density of 1.45 mW/cm^2 at 0.3 V, the OCV was 0.8 V, and the short-circuit current density was 11 mA/cm^2. Biofuel cells with these multilayer structures were then connected in series or in parallel. Such complex systems can generate power of over 100 mW, which was sufficient to successfully power a radio-controlled car or a memory-type Walkman player. Further, it was demonstrated that the Walkman and the radio-controlled car with this power supply could operate continuously for at least two hours. An additional advantage of the proposed device is that other fuels could be used if GDH is substituted by other appropriate dehydrogenases.

Analysis of biofuel cell operations can also be used to identify compounds that inhibit the enzymes on the electrodes or the general preparation of self-powered sensing devices. For example, in 2010, Dong and co-workers [161] developed a fully-integrated biofuel cell on a microprocessor and demonstrated its applicability for the determination of various cyanides, based on their effect on the power output of the biofuel cell. The system consisted of an anode coated with multilayers of CNTs, thionine, AuNPs, and GDH, and a cathode coated with multilayers of CNTs, PLL, and laccase. The initial OCV was 0.620 V and the power density was 302 μW/cm^2, but when cyanide was introduced into the analyte along with laccase inhibitor, the performance showed a linear response to cyanide in the range of 3.0×10^{-7} to 5.0×10^{-4} M. The detection limit (1.0×10^{-7} M) of this system is lower than the permissible concentration of cyanide in drinking water (1.9×10^{-6} M), according to the World Health Organisation (WHO). This self-powered sensor was successfully used to detect the cyanide concentration in a real cassava sample, which is the main source of carbohydrates in South America and Africa. Importantly, a self-powered biosensor connected with a resistor and a multimeter represents a simple device for the fast detection of cyanides in biological samples.

Zhang and co-workers [162] were the first to demonstrate a novel enzymatic fuel cell powered by maltodextrin and consisting of 3-enzymes in total. Both α-glucan (maltodextrin) phosphorylase (EC 2.4.1.1) and phosphoglucomutase (EC 2.7.5.1) were in solution, and the third component, glucose-6-phosphate dehydrogenase (G6PDH; EC 1.1.1.49), was immobilised on the carbon paper electrode coated with COOH-functionalised MWCNTs. In this system, maltodextrin phosphorylase and phosphoglucomutase convert the maltodextrin to glucose-6-phosphate (G6P), which is then oxi-

dised by the G6PDH immobilised on the anode. The cathode in this system is a diffusion electrode consisting of Nafion and a carbon cloth modified with Pt (0.5 mg/cm^2). When the G6P substrate concentration was 10 mM, a maximum power density of 60 μW/cm^2 was obtained and the cell maintained 42% of the output power after 11 days. When the substrate was changed to 40 mM maltodextrin, the maximum power density, 120 μW/cm^2 was obtained in 100 mM HEPES buffer containing 2 mM NAD^+. In terms of efficiency, using maltodextrin as a low-cost chemical fuel for the EFC resulted in an 11% larger chemical energy output (relative to the weight of the fuel), as compared with analogous glucose-air fuel cells.

Efficient conversion of the chemical energy stored in biomass, such as cellulose, into electrical energy, represents an important advancement in the development of biofuel cells. However, the high degree of crystallinity and poor solubility in water and most organic solvents fundamentally hinder the application of cellulose for energy production. A simple strategy was proposed by Mao and co-workers [163] which involves an important cellulose derivative, carboxymethylcellulose (CMC), which can easily be obtained from cellulose and has good solubility in water. The cellulase enzyme was used as the biocatalyst in the solution to catalyse the initial step of the procedure (hydrolysis of CMC to glucose), and the glucose produced was then used to generate electricity using fuel biogas. The bioanode consisted of GDH and MG adsorbed on SWCNTs to perform electrocatalytic NADH oxidation, and the cathode was coated with laccase that was also cross-linked on SWCNTs. In the presence of 10 mM NAD^+ in the hydrolysed CMC aerated solution, the OCV was 0.75 V, and a maximum power output of 128 μW/cm^2 was obtained at 0.35 V. These values are comparable or even higher than those achieved using other techniques to produce electricity from cellulose or cellulose derivatives.

Using multiple enzymes at a given electrode represents a way to transform cheaper fuels and/or obtain more power in the biofuel cell. Kondo and co-workers [164] presented an enzymatic biofuel cell employing three co-immobilised enzymes at the anode, including NAD-dependent GDH, NAD(P)-dependent gluconate-5-dehydrogenase (G5DH; EC 1.1.1.69), and diaphorase. Glucose was oxidised to gluconate by GDH, and in the following step, the gluconate was oxidised to 5-keto-gluconate using G5DH. The biocathode was a glassy carbon electrode covered with CNTs, BOD, 2,2′-azinobis(3-ethylbenzotha-zoline-6-sulphonic acid) (ABTS), and poly-allylamine glutaraldehyde. The fuel cell generated a maximum power density of 12.50 μW/cm^2 at 0.160 V, which is approximately 1.6 times larger than that achieved by the same authors using only two enzymes (GDH and Dp) co-immobilised on the anode.

Self-powered nanotechnology generates electricity from the environment for various applications in implantable biomedical devices, wireless sensors, and portable electronic devices. MacVittie and Katz [165] introduced a self-powered, electrochemical memristor, in which the logic network system involved a cascade of enzymes including maltose phosphorylase (MPh; EC 2.4.1.8), GDH, and G6PDH. The electrodes were coated with a pH-sensitive polymer, which allowed the flow of charge following the decrease in pH resulting from glucose oxidation. A corresponding deceleration of electron transfer occurred when the pH increased due to the production of water molecules during the reduction reactions at the cathode.

Yan and co-workers [166] constructed a self-powered, microfluidic analytical device for determining mercury ion (Hg^{2+}) concentrations. This device consisted of a glucose/O_2 biobattery with GDH and AuNPs at the anode, and a cathode coated with platinum nanoparticle-modified CNTs. To construct a self-powered Hg^{2+} sensor, an aptamer-specific oligonucleotide that captures Hg^{2+} was immobilised on the anode containing the NAD^+-dependent GDH-modified AuNPs. In the presence of Hg^{2+}, the aptamer was hybridised to the immobilised capture probe on the anode through an interaction with thymine (T; Hg^{2+}-T). The OCV of this biobattery was 0.85 V, and the maximum power density was 146.7 μW/cm^2 in the presence of 100 nM Hg^{2+}. Under optimal conditions, this self-powered sensor allows detection of Hg^{2+} at the picomolar level, therefore representing a good example of a portable, small-sized testing device to conduct quantitative tests at the point of care, without auxiliary instruments or electronics. Various other recognition elements, such as molecularly imprinted polymers, antibodies, and nucleic acids, can all be used in such devices.

Atanassov and co-workers [167] prepared a paper-based supercapacitive glucose/air biofuel cell assembled into a capillary-driven microfluidic system. The anode, made of NAD^+-dependent GDH mediated by methylene green immobilised in a CNT/CHIT matrix, was supplied with glucose by a capillary flow system. BOD deposited on teflonised buckypaper was used as the gas diffusion layer cathode, in order to promote the flow of oxygen to the catalytic active sites, and the paper-based system was loaded by itself at rest and discharged by high current pulses up to 4 mA/cm^2. The practical power of the system was 1.07 mW/cm^2 (13.1 mW), which is the highest power achieved using GDH as the anode enzyme, to date. In addition, the maximum power found with 0.01 s pulses was 0.87 mW/cm^2 (10.6 mW) at 4 mA/cm^2. This device takes advantage of the capacitive properties of the bioelectrodes, where the power output was optimised by more than an order of magnitude when the device operated in the pulsed mode. This design exemplifies a self-sufficient, environmentally-friendly, hybrid supercapacitor that can be used successfully for practical applications, such as sensors, biomedical devices, or other portable devices.

Katz and co-workers [168] constructed a biofuel cell based on the electrocatalytic NADH oxidation and H_2O_2 reduction. Carbon fibre electrodes functionalised with graphene nanoflakes were used as the electrode substrates, and meldola blue and GDH were adsorbed on the anode, while hemin and glucose oxidase (GOx; EC 1.1.3.4) were adsorbed on the cathode. The NADH and H_2O_2 were both formed *in situ*, and the NADH oxidation by MOB, and H_2O_2 reduction by hemin, led to the generation of current in the biofuel cell. The advantage of this system was that the biocatalytic electrodes function in the same solution without the need to separate the anodic and cathodic reactions (i.e., without a membrane separating the anode and cathode areas), because GDH is not sensitive to oxygen, and GOx is not sensitive to the presence of the NAD^+/NADH cofactor system. A representative biological solution that was similar to human serum consisted of 0.02 mM NAD^+ and 5 mM glucose, in a 0.1 M PBS solution at pH 7.0 with O_2 content in equilibrium with air. The biofuel cell generated power density of 18 μW/cm^2 with a load resistance of approximately 1 kΩ. In fact, when this system was tested in the presence of a human serum solution using naturally present NAD^+ and glucose, the power density was lower than in the model solution. This observation was a result of the lower concentration of NAD^+ and a much higher viscosity of human serum as compared with the aqueous biological model solutions. Two such biofuel cells connected in a series were shown to have the capability to power a watch.

Singhal and co-workers [169] recently used felt electrodes with electrolytically deposited PMG and GDH on SWCNTs as the bioanode. Preparation of the biocathode was conducted using MWCNTs with 1-pyrenebutanoic acid succinimidyl ester (PBSE), 2,5-dimethyl-1-phenyl-1H-pyrrolanohyde (Di-Carb), haematin, and BOD. This membrane-free biofuel cell showed a power density of 1.1 mW/cm^2 at pH 7.0 in a 100 mM glucose/10 mM NAD solution. A significant increase in current density was obtained by applying hematin to the biocathode surface, and this observation was ascribed to the resulting advantageous BOD orientation on the

hematin-modified electrode surface. In 2017, Karimi and co-workers [170] used guanine and ionic liquid-derived ordered mesoporous carbon (GIOMC) modified with AuNPs as a novel electrochemical platform for the immobilisation of GDH and construction of an NADH biosensor. GIOMC has good conductivity relative to other mesoporous carbon materials due to the guanine and ionic liquid carbon sources. The GIOMC/AuNPs/mercaptosuccinic acid/GDH integrated system demonstrates high bioelectrocatalytic activity towards glucose oxidation. In this case, mesoporous carbon modified with SO_3^- groups with immobilised BOD was used as the cathode, and in the membrane-free biofuel cell, the OCV was 0.508 V, the maximum power density was 33 μW/cm^2 at 0.257 V, and the maximum current density was 0.233 μA/cm^2.

Visible-Light-Enhanced BFCs have been another promising subject of active research in recent years, however NAD(P)-dependent GDH was only used in a few of these studies. Song and co-workers [171] prepared a BFC-supported immunosensor using visible light in combination with an electrochemical immunosensor. The BFC immunosensor was used for sensitive detection of the carbohydrate antigen 15–3 (CA15-3). The paper electrode modified with bimetallic gold-silver nanoparticles and GDH was employed as the bioanode, and a photoreactive conductive polymer, poly-(terthiophene) (pTTh), was applied as the catalyst on the cathode to reduce oxygen after visible light illumination. A maximum power density of 70.2 μW/cm^2 and an OCV of 0.61 V were obtained when the supporting electrolyte was irradiated by visible light. This simple, effective and sensitive device showed acceptable, reproducible precision for detecting CA15-3. Accurate detection of other biological molecules should theoretically also be possible using this type of device. Amao and Shuto [172] constructed a visible light-operated CO_2-glucose biofuel cell with a Nafion membrane as the separator. In this case, the solution in the biofuel cell contained glucose, GDH, and NAD^+, and the anode was constructed by chlorin-e_6 immobilisation on a TiO_2 thin layer film on an optically transparent conductive glass electrode (OTE). The cathode was OTE with co-immobilised formate dehydrogenase and viologen with a long alkyl chain. Under visible light irradiation, CO_2 was reduced to produce formic acid and generate electricity. The short-circuit photocurrent, the OCV, and the maximum power density of this cell were 37 μA/cm^2, 0.390 V, and 57 μW/cm^2, respectively. The overall photoenergy conversion efficiency was 0.057%, and after 2 h of irradiation, 0.65 μmol of formic acid was produced in the cell.

The development of new biofuel cell systems based on GDH, is often highly focused on their potential biological and medical applications. For example, Nishizawa and co-authors [173] presented a biofuel cell comprised of a needle bioanode with GDH, and a biocathode with BOD, and inserted it into the vein of a rabbit ear (Fig. 4). Specifically, the bioanode was covered with GDH, Dp, PLL-modified vitamin K3, and PLL-modified NAD^+, and the cathode was Toray carbon paper with ketjenblack(KB)/poly (tetrafluoroethylene) (PTFE), and BOD. This biofuel cell was partially placed in the rabbit's ear by subcutaneous bioanode implantation, and the breathable biocathode took oxygen from the air. The maximum power of the cell was 0.42 μW at 0.56 V, and the OCV was 0.81 V. The compiled details regarding the GDH-based biofuel cells and biobatteries discussed in this review are shown in Table 3.

5. Perspectives

The common, commercially available glucose 1-dehydrogenases were isolated from *Prokarya* organisms or *Prokarya* hosts (*E. coli*) after heteroexpression of different bacterial genes. The proteins synthesised in these expression systems often cannot be glycosylated, and the non-glycosylated therapeutic protein market is related to the main host cell factory (*E. coli)* that generates approximately 30% of the 151 recombinant therapeutics [179]. Almost all NAD(P)-dependent GDH systems described in the literature that are isolated from mammalian sources (e.g., *Homo sapiens*, *Bos taurus*) are glycoproteins [38] or lipoproteins [15]. Post translational modifications are very important for correct folding of the native protein [180,181], stability of the protein molecular structure, and overall enzyme activity [182]. They are also related to the appropriate pH and optimal temperature for enzyme function [183]. It would be interesting to obtain the mammalian GDH mentioned above following heteroexpression in

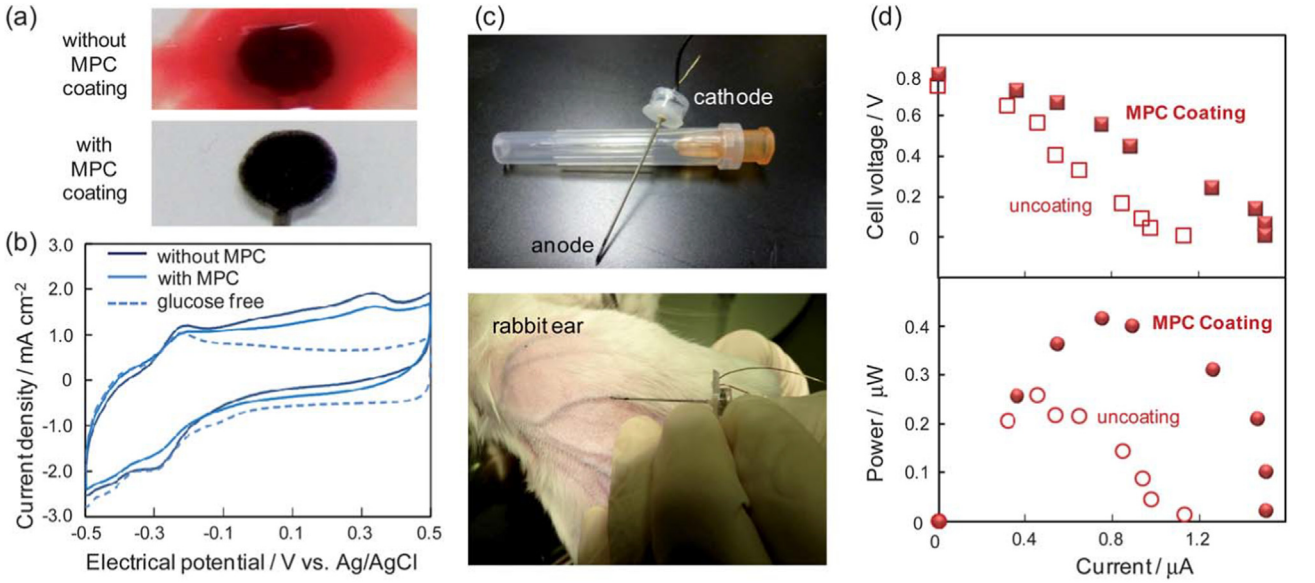

Fig. 4. (a) Photographs of electrode substrates with (and without) a 2-meth-acryloyloxyethyl phosphorylcholine (MPC)-polymer coating, taken after soaking in withdrawn blood for 2 h. (b) Cyclic voltammograms of bare and MPC-coated needle bioanodes at 10 mV s^{-1} in phosphate buffer containing 10 mM glucose. The control experiment (glucose-free) is also shown. The current density was estimated from the geometric area of the anodic peak (0.0032 cm^2). (c) Photographs of the assembled biofuel cell for power generation from a rabbit vein. (d) Performance of the biofuel cells using a needle anode, with and without MPC-coating, taken by inserting the needle anodes into a rabbit vein. Reprinted with permission from ref [173].

Table 3
Examples of GDH-based biofuel cells and biobatteries.

Anode enzyme, Electrode	Cathode enzyme, Electrode	P_{max} (μW/cm^2) (E (V))	OCV (V)	Conditions	Year/ Ref
GDH (from *Bacillus megaterium*), MOB, GLD	Pt	175.0 (0.560)	0.56	O_2 saturated 0.25 M phosphate buffer (pH 7.0), 80 mM glucose, 0.3 mM NADH	1985 [174]
GDH (from *Bacillus* sp.), Dp, PAA-VK3, KB, PLL	Pt, PDMS	14.5 (0.36)	0.62	air saturated PBS (pH 7.0), 0.5 mM NADH, 10 mM glucose	2005 [142]
GDH, PMB, SWCNTs, GLD	Lc (E.C. 1.10.3.2, from *T. versicolor)*, SWCNTs,	9.5 (0.52)	0.8	air saturated 0.10 M phosphate buffer pH 6.0, 10 mM NAD^+ and 30 mM glucose	2006 [143]
GDH, SWCNTs, NB, $NADP^+$, GLD	BOD, SWCNTs, GLD	23 (0.3)	0.7	O_2 saturated, 0.10 M phosphate buffer (pH 7.0), 40 mM glucose,	2007 [96]
GDH, PLL-VK3, Dp, KB	Pt, PDMS	32 (0.29)	0.55	air saturated phosphate-buffere (pH 7.0), 5.0 mM glucose, 1.0 mM NAD^+	2007 [152]
GDH (from *Aspergillus niger*), PBCB, SWNCTs, GLD	BOD (E.C.1.10.3.2, from *M. verrucaria*), SWCNTs, GLD	53.9 (0.50)	0.63	O_2 saturated 0.10 M phosphate (pH 7.0), 10 mM NAD^+, 40 mM glucose	2007 [150]
GDH (from *Thermoplasma acidophilum,* recombinant expressed in *E coli)*, 3DOM	Lc (E.C. 1.10.3.2, from *T. versicolor)*, 3DOM	178 (0.226)	0.32	air-saturated 0.1 M PBS (pH 6.0), 5 mM NADH, 30 mM glucose,	2008 [157]
GDH, MWCNTs, THN, AuNPs	Lc (EC 1.10.3.2, *T. versicolor*), PLL, MWCNTs	329 (0.470)	0.7	air saturated 0.1 M PBS (pH 6.0), 10 mM NADH, 30 mM glucose	2008 [158]
GDH (from *Thermoplasma acidophilum*), CNTs, NAD^+	Lc (E.C. 1.10.3.2, *Rhus vernificera*), CNTs	3.52 μW/m^3	–	air saturated PBS (pH 7.4), 5 mM glucose	2009 [175]
GDH (from *Pseudomonas* sp.), SWCNTs, PMB, GLD	BOD (E.C.1.3.3.5, from *M. verrucaria)*, SWCNTs, GLD	52 (0.3)	0.6	air saturated 0.10 M phosphate buffer (pH 7.0), 10 mM NAD^+, 40 mM glucose	2009 [151]
GDH, NAD^+, KB	BOD (EC 1.3.3.5), KB	52 (0.3)	0.642	O_2 saturated PBS, 50 mM glucose	2009 [153]
GDH (from *Bacillus* sp.*),* PLL, Dp, NADH, VK3, PAANa	BOD (EC 1.3.3.5, from *Myrothecium* sp.), $K_3[Fe(CN)_6]$, PLL	1450 (0.3)	0.8	air saturated 1.0 M PBS (pH 7.0), 0.4 mg glucose	2009 [160]
GDH (from *Thermoplasma acidophilum,* recombinant expressed in *E. coli)* MWCNTs, THN, AuNPs	Lc (EC 1.10.3.2, *T. versicolor*), MWCNTs, PLL	302 (0.4)	0.62	O_2 saturated 0.2 M PBS (pH 6.5), 10 mM NADH, 40 mM glucose	2010 [161]
GDH, CHIT, PMB, SWNHs	TiO_2–PtNPs	10.74 (0.275)	0.43	PBS (pH 7.0), 30 mM glucose, 10 mM NAD^+	2010 [176]
GDH (from *Bacillus* sp.), NB, SWCNTs-COOH, NAD^+, CA, GLD	Lc (from *Thermus thermophilus*), MG, SWCNTs, GLD	32.0 (0.32)	0.85	O_2 saturated 0.1 M PBS (pH 6.0), 10 mM NAD^+, 40 mM glucose, salt bridge	2011 [103]
GDH, SWNHs, MOB, GLD	BOD (E.C. 1.3.3.5, from *M. verrucaria*), SWNHs, GLD	140 (0.51)	0.72	air saturated 0.10 M PBS (pH 7.0), 10 mM NAD^+, 30 mM glucose	2011 [146]
GDH, maltodextrin phosphorylase, phosphoglucutase, glucose-6-phosphate dehydrogenase, Dp, VK3	Pt, CF	120 (0.26)	0.34	air saturated 100 mM HEPES buffer, 2 mM NAD^+, 40 mM maltodextrin, Nafion membrane	2011 [162]
GDH (from microorganism), Dp, PLL-VK3, PLL-NAD^+	BOD (EC 1.3.3.5, from *Myrothecium* sp.), KB, PTFE	0.42 (0.56)	0.81	mixture in a vein of a rabbit ear	2011 [173]
GDH (from *Pseudomonas* sp.), MG, SWCNTs, GLD	Lc (E.C.1.10.3.2, from *T. versicolor*), SWCNTs, GLD	128 (0.35)	0.75	air saturated 0.5 mg/ml cellulose, 1 wt%. a solution of CMC, 0.10 M acetate buffer (pH 5.5), 10 mM NAD^+	2012 [163]
GDH (from *T. acidophilum*), SWCNTs, cubic phase	Lc, SWCNTs-NAPH	131 (0.30)	0.55	0.15 M McIlvaine buffer (pH 6.0), 5 mM NAD^+, 80 mM glucose	2012 [177]
GDH (from *Thermoplasma acidophilum)*, MWCNTs, PMB, GLD	iodide/tri-iodide redox couple	2.43 (0.363)	0.42	anodic chamber: PBS (pH 7.0), 200mM glucose, 10 mM NAD^+, cathodic chamber: PBS (pH 7.0), 50 mM iodide, 5 mM iodine	2012 [178]
GDH, Ga5DH, $NAD(P)^+$, Dp, SWCNTs-Fc, PAA, GLD	BOD (from *M. verrucaria)*, SWCNTs, ABTS, PAA, GLD	12.50 (0.160)	0.55	O_2 saturated 0.1 M phosphate buffer (pH 7.2), 100 mM glucose.	2013 [164]
GDH (from *T. acidophilum*), Au@Ag BMPs	pTTh	70.2 (0.41)	0.61	air saturated 10.0 mM PBS (pH 7.0), 10 mM NAD^+/NADH, 50 mM glucose	2015 [171]
GDH (from *Pseudomonas* sp.), NB, MWCNTs-NH2, PAMAM-Den	BOD (E.C.1.3.3.5, from *M. verrucaria*,), DNA, MWCNTs	45 (0.428)	0.66	O_2 saturated 0.1 M PBS (pH 7.0), 10 mM NAD^+, 50 mM glucose	2015 [144]
TiO_2, Chl	FDH, VG	57 (0.2)	0.390	CO_2 saturated 10 mM Tris-HCl buffer (pH 7.0), 0.1 M glucose, 3.5 mM NAD^+, 10 μM GDH (*Bacillus sp.*),	2015 [172]
GDH, [Ni(phendion) (phen)]Cl_2, MWCNTs-COOH,	BOD, MWCNTs, AuNPs	40 (0.284)	0.520	O_2 saturated 0.1 M PBS (pH 7.0), 10 mM NAD^+, 100 mM glucose	2015 [116]
GDH (from *T. acidophilum*), AuNPs	PtNPs-CNTs	146.7 (0.48)	0.85	air saturated 0.10 M PBS (pH 7.0), 10 mM NAD^+/NADH, 30 mM glucose	2015 [166]
GDH, MG, MWCNTs, CHIT	BOD, BP, TCB	1070 (0.268)	0.60	air saturated 0.1 M PBS (pH 7.5) 0.1 M glucose, 1 mM NAD^+, 0.1 M KCl	2016 [167]
GDH, LPEI-NQ	Lc, MWCNTs-ANT	123.2 (0.046)	0.767	anodic chamber: 0.2 M citrate /phosphate buffer (pH 6.5), 200 mM glucose, 10 mM NAD^+, cathodic chamber: O_2 saturated 0.2 M citrate /phosphate buffer (pH 5.5).	2016 [148]

(*continued on next page*)

Table 3 (*continued*)

Anode enzyme, Electrode	Cathode enzyme, Electrode	P_{max} (μW/cm^2) (E (V))	OCV (V)	Conditions	Year/ Ref
GDH (from *Pseudomonas* sp.), GCF, MOB	GOx (E.C. 1.1.3.4, from *Aspergillus niger*), GCF, hemin	18 (0.078)	0.500	air saturated 0.1 M PBS (pH 7.0), 0.2 mM NAD^+, 5 mM glucose	2017 [168]
GDH (from *Pseudomonas* sp.), GIOMC, AuNPs	BOD (E.C. 1.3.3.5, from *M. verrucaria*), IOMC-PhSO3H, AuNPs	33 (0.257)	0.508	O_2 saturated 0.1 MPBS (pH 7.0), 10 mM NAD^+, 50 mM glucose	2017 [170]
GDH, BPV-LPEI, Dp	Lc, MWCNTs-ANT	31.3 (0.756)	1.1	anodic chamber: 0.1 M phosphate–citrate buffer (pH 7.0), 5 mM NAD^+, 100 mM glucose, cathodic chamber: air saturated 100 mM citrate/phosphate buffer (pH 7.0)	2017 [149]
GDH (from *Pseudomonas* sp.), PMG, SWCNTs	BOD (EC 1.3.3.5, from *M. verrucaria*.), MWCNTs, PBSE, Di-Carb	1100 (0.300)	0.7	air saturated 245 mM PBS (pH 7.0), 100 mM glucose, 10 mM NAD^+	2018 [169]
GDH, Dp, NADH, VK3	BOD, $K_3[Fe(CN)_6]$	211 (0.360)	0.6	O_2 saturated 50 mM phosphate buffer (pH 7.0), 5 mM glucose	2019 [159]

Abbreviations: single walled carbon nanotubes (SWCNTs), multi-walled carbon nanotubes (MWCNTs), carbon nanotubes (CNTs), COOH-functionalized SWCNTs (SWCNTs-COOH), amine functionalized multiwall carbon nanotubes (MWCNTs-NH_2), graphite rods (GR), meldola blue (MOB), toluidine blue (TB), chitosan (CHIT), polyethyleneimine (PEI), poly[N,N'-(sulpho-p-phenylene) terephthalamide] (SPPT), gentamicin (GTN), tris(2,2′-bipyridyl)ruthenium(II) ($Ru(bpy)_3^{2-}$), Eastman AQ (EAQ), Nafion (Nf), poly-toluidine blue (PTB), chitosan (CHIT), glutaraldehyde (GLD), 3,4-dihydroxybenzaldehyde (3,4-DHB), diaphorase (Dp), carbon nanotube paste (CNTP), poly(1-vinylimidazole)$_{12}$-[osmium(4,4′-dimethyl-2,2′-dipyridyl)$_2Cl_2$]$^{2+/+}$ (Os redox polymer), nile blue (NB), poly-nile blue (PNB), thionine (THN), gold nanoparticles (AuNPs), plasma-polymerized thin film (PPF), screen-printed carbon electrode (SPCE), cellulose acetate (CA), methylene green (MG), 1-butyl-3-methylimidazolium glycine ($Bmim^+Gly^-$), tris(2,2′-bipyridyl) ruthenium(II) chloride hexahydrate ($Ru(bpy)_3^{2+}$), mesoporous silica sol–gel (MPSG), Resydrol (Resy), polyethylene glycol 400 (PEG-400), poly(phenosafranin)-functionalized single-walled carbon nanotubes (SWCNTs-PPS), 1-butyl-3-methylimidazolium hexafluorophosphate ionic liquid (BMIMPF6) IL, phenothiazine (PT), plasma-polymerized thin film (PPF), reduces graphene oxide (RGO), 5-[2,5-di(thiophen-2-yl)-1H-pyrrol-1-yl]-1,10-phenanthroline iron(III) chloride (FePhenTPy), zeolitic imidazolate frameworks (ZIFs), methylene green (MG), safranin (SAF), amine-derivative multiwalled carbon nanotubes (MWCNTs-NH_2), carboxylated polyamidoamine dendrimer (PAMAM-Den), CdS quantum dots (CdS QDs), 1-pyrene butyric acid (PBA), 5-(2,5 di(thiophen-2-yl)-1H–pyrrol-1-yl)-1,10-phenanthroline iron(III) chloride (Fe-PhenTPy), hematoxylin film (PHT), 1,10-phenanthroline-5,6-dione and 5-amino-1,10-phenanthrolin ([Ni(phendion)(phen)]Cl_2, hybrid ZnS–CdS quantum dots (ZnS–CdS QDs), mercapto acetic acid (MAA), iron (II) sulphide (FeS), iron disulphide (FeS_2), iron(III) sulphide (Fe_2S_3), Greigite (Fe_3S_4), pyrroloquinoline quinone (PQQ), 3-aminophenyl boronic acid monohydrate (APB), cystamine (Cys), methylene blue (MB), ketjenblack (KB), poly methylene blue (PMB), nanoporous gold (NPG), bis(2,2-bipyridyl)dichloroosmium(II) [Os(bpy)2Cl_2], poly (vinylacetate)-poly(ethylene)-copolymer (PVAc), poly(pyrrole) (PPy), 3-naphthoquinonesulphonate (NQS), carbon paste (CP), Os(4,4′-dimethyl, 2,2′-bipyridine)$_2$(l,10-phenanthroline-5,6-dione (osphendione), bls(benzophenoxazinyl) derivative of benzene-1,4-dicarboxamide (BPT), p-methylamino-phenolsulphate (MAP), 1-pyrenebutanoic acid succinimidyl ester (PBSE), 2,5-dimethyl-1-phenyl-1H-pyrrole-3-carbaldehyde (Di-Carb), gold−silver bimetallic nanoparticles (Au@Ag BMPs).

eukaryotic hosts in order to evaluate their redox properties using electrochemical methods. To date, expression in eukaryotic hosts is mainly limited to *Saccharomyces cerevisiae*, *Pichia pastoris*, and *Aspergillus* systems [184,185].

The nicotinamide redox cofactors ($NAD(P)^+$) play important roles in biological electron transfer, however there are certain difficulties related to using them in various applications that are connected to their chemical properties. First, the reduced and oxidised forms of nicotinamide cofactors are subject to decomposition in aqueous solution. The reduced forms of these cofactors are stable in base but labile in acid, and the oxidised forms are stable in acid but labile in base [67]. The decomposition of NADPH reflects an additional intramolecular acid catalysis by the 2′-phosphate group [69], and the most effective, general acid catalysts are those with a pK_a approximately equal to the solution pH. The half-lives for the reduced forms (i.e., NADH and NADPH) in 0.1 M sodium phosphate at pH 7 are 27 and 13 h, respectively, however these properties can be modified by appropriate protein engineering techniques including polymerisation, hydrophobisation, or hydrophilisation processes, which may change physical–chemical and kinetic properties of the proteins [186,187]. A related disadvantage of these nicotinamide cofactors originates from the fact that they are not covalently bound to the enzyme and can therefore readily dissociate (K_D = 10^{-3}-10^{-5} M). The exchange of NAD or NADP for purposefully modified analogues is another way to improve the cofactor attachment to the enzyme body. Some NAD^+ analogues are already employed as anticancer substances [186] or enzyme inhibitors (e.g., NAD^+ kinase, Lysine acetyltransferases) [187]. They can also serve to shift the reduction potential of various enzymes, as in the case of complexation with nitrate dehydrogenase [188], alcohol dehydrogenase (from horse liver), sorbitol dehydrogenase (from sheep liver), glucose-6-phosphate dehydrogenase (from *Leuconostoc mesenteroides*), and glucose dehydrogenase (from *Bacillus megaterium*) [189]. The electrochemical characterisation of various NAD^+ analogues has been described in the literature [190–192].

As presented in this review, challenges for successful implementation of biofuel cells include increasing the stability of NAD^+ and $NADP^+$, and improving the binding of these cofactors in the GDH enzyme. Currently, state-of-the-art fuel cells containing $NAD(P)^+$-dependent GDH usually need an additional unbound cofactor supply from the solution. If the cofactor could be encapsulated in a small volume close to the enzyme or connected via a small linker into the carrier matrix, its re-oxidation could be facilitated. Such an encapsulation together with the enzyme could be more effective for improving the fuel cell efficiency relative to the direct electrode binding schemes presented in this review. Replacing the original cofactor in the enzyme molecule with a novel, modified nicotinamide cofactor analogue would also help to retain the enzyme activity and make the NAD^+- and $NADP^+$-dependent enzymes more attractive for applications in fuel cells and sensing devices. A combination of biochemical and electrochemical research is required in order to explore such approaches. Currently, although numerous applications of NAD^+- and $NADP^+$-dependent GDH have been reported, anodes based on PQQ- or FAD-dependent proteins are still generally preferred for bioelectrodes and biofuel cell devices.

Declaration of Competing Interest

The authors declare that they have no known competing financial interests or personal relationships that could have appeared to influence the work reported in this paper.

Acknowledgements

This work was supported by grants from the University of Warsaw and Maria Curie Sklodowska University.

References

[1] K. Matsushita, H. Toyama, O. Adachi, Respiratory chains and bioenergetics of acetic acid bacteria, Advan. Microbial. Phys. 36 (1994) 247–301, https://doi.org/10.1016/s0065-2911(08)60181-2.
[2] J.P. Klinman, F. Bonnot, Intrigues and intricacies of the biosynthetic pathways for the enzymatic quinocofactors: PQQ, TTQ, CTQ, TPQ, and LTQ, Chem. Rev. 114 (2014) 4343–4365, https://doi.org/10.1021/cr400475g.
[3] C. Anthony, Bacterial Energy Transduction, in: C. Anthony (Ed.), Acad. Press, San Diego, 1988, pp. 1–400. ISBN: 0-12-058815-3.
[4] O. Adachi, D. Moonmangmee, D. Toyama, M. Yamada, E. Shingawa, K. Matsushita, New developments in oxidative fermentation, Appl. Microbiol. Biotechnol. 60 (2003) 643–653, https://doi.org/10.1007/s00253-002-1155-9.
[5] U. Deppenmeier, M. Hoffmeister, C. Prust, Biochemistry and biotechnological applications of *Gluconobacter strains*, Appl. Microbiol. Biotechnol. 60 (2003) 233–242, https://doi.org/10.1007/s00253-002-1114-5.
[6] J. Tkac, J. Svitel, I. Vostiar, M. Navratil, P. Gemeiner, Membrane-bound dehydrogenases from *Gluconobacter* sp. Interfacial electrochemistry and direct bioelectrocatalysis, Bioelectrochem. 76 (2009) 53–62, https://doi.org/10.1016/j.bioelechem.2009.02.013.
[7] T. Pongtharangkul, P. Chuekitkumchorn, N. Suwanampa, P. Payongsri, K. Honda, W. Panbangred, Kinetic properties and stability of glucose dehydrogenase from *Bacillus amyloliquefaciens* SB5 and its potential for cofactor regeneration, AMB Express. 5 (2015) 68, https://doi.org/10.1186/s13568-015-0157-9.
[8] S.H. Baik, F. Michel, N. Aghajari, R. Haser, S. Harayama, Cooperative effect of two surface amino acid mutations (Q252L and E170K) in glucose dehydrogenase from *Bacillus megaterium* IWG3 on stabilization of its oligomeric state, Appl. Environ. Microbiol. 71 (2005) 3285–3293, https://doi.org/10.1128/AEM.71.6.3285-3293.2005.
[9] Z. Xu, K. Jing, Y. Liu, P. Cen, High-level expression of recombinant glucose dehydrogenase and its application in NADPH regeneration, J. Ind. Microbiol. Biotechnol. 34 (2007) 83–90, https://doi.org/10.1007/s10295-006-0168-2.
[10] N. Strauss, Role of glucose dehydrogenase in germination of *Bacillus subtilis* spores, FEMS Microbiol. Lett. 20 (1983) 379–384, https://doi.org/10.1111/j.1574-6968.1983.tb00152.x.
[11] E. Vázquez-Figueroa, J. Chapparro-Riggers, A.S. Bommarius, Development of a thermostable glucose dehydrogenase by a structure-guided consensus concept, ChemBioChem. 8 (2007) 2295–2301, https://doi.org/10.1002/cbic.200700500.
[12] Y. Kobayashi, H. Ueyama, K. Horikoshi, NAD-dependent maltose dehydrogenase and NAD-dependent D-glucose dehydrogenase of alkalophilic *Corynebacterium sp.* no. 150–1, Agric. Biol. Chem. 44 (1980) 2837–2841, https://doi.org/10.1080/00021369.1980.10864421.
[13] O. Adachi, K. Matsushita, E. Shinagawa, M. Ameyama, Crystallization and characterization of NADP-dependent D-glucose dehydrogenase from *Gluconobacter suboxydans*, Agric. Biol. Chem. 44 (1980) 301–308, https://doi.org/10.1080/00021369.1980.10863953.
[14] H. Ding, F. Gao, D. Liu, Z. Li, X. Xu, M. Wu, Y. Zhao, Significant improvement of thermal stability of glucose 1-dehydrogenase by introducing disulfide bonds at the tetramer interface, Enzyme Microb. Technol. 53 (2013) 365–372, https://doi.org/10.1016/j.enzmictec.2013.08.001.
[15] D.P. Campbell, W.R. Carper, R.E. Thompson, Bovine liver glucose dehydrogenase: Isolation and characterization, Arch. Biochem. Biophys. 215 (1982) 289–301, https://doi.org/10.1016/0003-9861(82)90307-1.
[16] A.S.L. Hu, A.L. Cline, The regulation of some sugar dehydrogenases in a pseudomonad, BBA – Gen. Subj. 93 (1964) 237–245, https://doi.org/10.1016/0304-4165(64)90371-X.
[17] G. Avigad, Y. Alroy, S. Englard, Purification and properties of a nicotinamide adenine dinucleotide phosphate-linked aldohexose dehydrogeanse from *Gluconobacter cerinus*, J. Biol. Chem. 243 (1968) 1936–1941.
[18] M.A. Ruggiero, D.P. Gordon, T.M. Orrell, N. Bailly, T. Bourgoin, R.C. Brusca, T. Cavalier-Smith, M.D. Guiry, P.M. Kirk, A higher level classification of all living organisms, PLoS One 10 (2015) e0119248, https://doi.org/10.1371/journal.pone.0119248.
[19] P. Haferkamp, S. Kutschki, J. Treichel, H. Hemeda, K. Sewczyk, D. Hoffmann, M. Zaparty, B. Siebers, An additional glucose dehydrogenase from *Sulfolobus solfataricus*: fine-tuning of sugar degradation?, Biochem. Soc. Trans. 39 (2011) 77–81, https://doi.org/10.1042/bst0390077.
[20] P. Haferkamp, Biochemical studies of enzymes involved in glycolysis of the thermoacidophilic crenarchaeon Sulfolobus solfataricus, 2011. urn:nbn:de:hbz:464-20111205-141330-9.
[21] C.C. Milburn, H.J. Lamble, A. Theodossis, S.D. Bull, D.W. Hough, M.J. Danson, G. L. Taylor, The structural basis of substrate promiscuity in glucose dehydrogenase from the hyperthermophilic archaeon *Sulfolobus solfataricus*, J. Biol. Chem. 281 (2006) 14796–14804, https://doi.org/10.1074/jbc.M601334200.
[22] T. Ohshima, Y. Ito, H. Sakuraba, S. Goda, Y. Kawarabayasi, The *Sulfolobus tokodaii* gene ST1704 codes highly thermostable glucose dehydrogenase, J. Mol. Catal. B Enzym. 23 (2003) 281–289, https://doi.org/10.1016/S1381-1177(03)00091-2.
[23] L.D. Smith, N. Budgen, S.J. Bungard, M.J. Danson, D.W. Hough, Purification and characterization of glucose dehydrogenase from the thermoacidophilic archaebacterium *Thermoplasma acidophilum*, Biochem. J. 261 (1989) 973–977, https://doi.org/10.1042/bj2610973.
[24] Y. Nishiya, N. Tamura, T. Tamura, Analysis of bacterial glucose dehydrogenase homologs from thermoacidophilic archaeon *Thermoplasma acidophilum*: Finding and characterization of aldohexose dehydrogenase, Biosci. Biotechnol. Biochem. 68 (2004) 2451–2456, https://doi.org/10.1271/bbb.68.2451.
[25] B. Siebers, V.F. Wendisch, R. Hensel, Carbohydrate metabolism in *Thermoproteus tenax*: *In vivo* utilization of the non-phosphorylative Entner-Doudoroff pathway and characterization of its first enzyme, glucose dehydrogenase, Arch. Microbiol. 168 (1997) 120–127, https://doi.org/10.1007/s002030050477.
[26] V.M. Gumerov, A.V. Mardanov, A.V. Beletsky, M.I. Prokofeva, E.A. Bonch-Osmolovskaya, N.V. Ravin, K.G. Skryabin, Complete genome sequence of "*Vulcanisaeta moutnovskia*" strain 768–28, a novel member of the hyperthermophilic crenarchaeal genus *Vulcanisaeta*, J. Bacteriol. 193 (2011) 2355–2356, https://doi.org/10.1128/JB.00237-11.
[27] T. Nishioka, Y. Yasutake, Y. Nishiya, T. Tamura, Structure-guided mutagenesis for the improvement of substrate specificity of *Bacillus megaterium* glucose 1-dehydrogenase IV, FEBS J. 279 (2012) 3264–3275, https://doi.org/10.1111/j.1742-4658.2012.08713.x.
[28] H.E. Pauly, G. Pfleiderer, D-glucose dehydrogenase from *Bacillus megaterium M 1286*: purification, properties and structure, Hoppe-Seyleŕs Z, Physiol. Chem. 356 (1975) 1613–1624, https://doi.org/10.1515/bchm2.1975.356.2.1613.
[29] Y. Fujita, R. Ramaley, E. Freese, Location and properties of glucose dehydrogenase in sporulating cells and spores of *Bacillus subtilis*, J. Bacteriol. 132 (1977) 282–293. http://jb.asm.org/.
[30] R.F. Ramaleyz, N. Vasanthaq, Glycerol protection and purification of *Bacillus subtilis* glucose dehydrogenase, J. Biol. Chem. 258 (1983) 12558–12565. http://www.jbc.org/.
[31] F. Gao, H. Ding, X. Xu, Y. Zhao, A self-sufficient system for removal of synthetic dye by coupling of spore-displayed triphenylmethane reductase and glucose 1-dehydrogenase, Environ. Sci. Pollut. Res. 23 (2016) 21319–21326, https://doi.org/10.1007/s11356-016-7330-9.
[32] N. Boontim, K. Yoshimune, S. Lumyong, M. Moriguchi, Purification and characterization of D-glucose dehydrogenase from *Bacillus thuringiensis* M15, Ann. Microbiol. 54 (2004) 481–492.
[33] Y. Kobayashi, H. Ueyama, K. Horikoshi, Comparative studies of NAD^+ - dependent maltose dehydrogenase and D-glucose dehydrogenase produced by two strains of alkalophilic *Corynebacterium* species, Agric. Biol. Chem. 46 (1982) 2139–2142, https://doi.org/10.1080/00021369.1982.10865397.
[34] Y. Kobayashi, K. Horikoshi, Purification and properties of NAD-dependent D-glucose dehydrogenase produced by alkalophilic *Corynebacterium sp*, No. 93–1, Agric. Biol. Chem. 44 (1980) 2261–2269, https://doi.org/10.1080/00021369.1980.10864318.
[35] H.T. Ding, Y.Q. Du, D.F. Liu, Z.L. Li, X.J. Chen, Y.H. Zhao, Cloning and expression in *E. coli* of an organic solvent-tolerant and alkali-resistant glucose 1-dehydrogenase from *Lysinibacillus sphaericus* G10, Bioresour. Technol. 102 (2011) 1528–1536, https://doi.org/10.1016/j.biortech.2010.08.018.
[36] Y. Yang, B. Wei, Y. Zhao, J. Wang, Construction of an integrated enzyme system consisting azoreductase and glucose 1-dehydrogenase for dye removal, Bioresour. Technol. 130 (2013) 517–521, https://doi.org/10.1016/j.biortech.2012.12.106.
[37] M.A. Tranulis, B. Christophersen, B. Borrebaek, Glucose dehydrogenase in beef (*Bos taurus*) and rainbow trout (*Oncorhynchus mykiss*) liver: a comparative study, Comp. Biochem. Physiol. - Part B Biochem. 109 (1994) 427–435, https://doi.org/10.1016/0305-0491(94)90025-6.
[38] S. Senesi, M. Csala, P. Marcolongo, R. Fulceri, J. Mandl, G. Banhegyi, A. Benedetti, Hexose-6-phosphate dehydrogenase in the endoplasmic reticulum, Biol. Chem. 391 (2010) 1–8, https://doi.org/10.1515/BC.2009.146.
[39] E.P. Gomez-Sanchez, M.T. Gomez-Sanchez, A.F. de Rodriguez, D.G. Romero, M. P. Warden, M.W. Plonczynski, C.E. Gomez-Sanchez, Immunohistochemical demonstration of the mineralocorticoid receptor, 11β-hydroxysteroid dehydrogenase-1 and -2, and hexose-6-phosphate dehydrogenase in rat ovary, J. Histochem. Cytochem. 57 (2009) 633–641, https://doi.org/10.1369/jhc.2009.953059.
[40] W.R. Carper, D.P. Campbell, S.W. Morrical, R.E. Thompson, Characterization studies of glucose dehydrogenase, Experientia 39 (1983) 1295–1297, https://doi.org/10.1007/BF01990378.
[41] A. Bairoch, R. Apweiler, The SWISS-PROT protein sequence database and its supplement TrEMBL in 2000, Nucleic Acids Res. 28 (2000) 45–48, https://doi.org/10.1093/nar/28.1.45.
[42] J. Sambrook, D.W. Russell, Molecular cloning: A laboratory manual, 3rd ed., in: J. Argentine, N. Irwin (Eds.), Cold Spring Harbor, New York, 2001.
[43] H. Yun, H.L. Choi, N.W. Fadnavis, B.G. Kim, Stereospecific synthesis of (R)-2-hydroxy carboxylic acids using recombinant *E. coli* BL21 overexpressing YiaE from *Escherichia coli* K12 and glucose dehydrogenase from *Bacillus subtilis*, Biotechnol. Prog. 21 (2005) 366–371, https://doi.org/10.1021/bp049694w.
[44] Y. Makino, S. Negoro, I. Urabe, H. Okada, Stability-increasing mutants of glucose dehydrogenase from *Bacillus megaterium* IWG3, J. Biol. Chem. 264 (1989) 6381–6385.

[45] J. Hyun, M. Abigail, J.W. Choo, J. Ryu, H.K. Kim, Effects of N-/C-terminal extra tags on the optimal reaction conditions, activity, and quaternary structure of *Bacillus thuringiensis* glucose 1-dehydrogenase, J. Microbiol. Biotechnol. 26 (2016) 1708–1716, https://doi.org/10.4014/jmb.1603.03021.

[46] A. Theodossis, C.C. Milburn, N.I. Heyer, H.J. Lamble, D.W. Hough, M.J. Danson, G.L. Taylor, Preliminary crystallographic studies of glucose dehydrogenase from the promiscuous Entner-Doudoroff pathway in the hyperthermophilic archaeon *Sulfolobus solfataricus*, Acta Crystallogr. Sect. F Struct. Biol. Cryst. Commun. 61 (2005) 112–115, https://doi.org/10.1107/S174430910403101X.

[47] P. Giardina, M.G. de Biasi, M. de Rosa, A. Gambacorta, V. Buonocore, Glucose dehydrogenase from the thermoacidophilic archaebacterium *Sulfolobus solfataricus*, Biochem. J. 239 (1986) 517–522, https://doi.org/10.1042/bj2390517.

[48] S.R. Bhaumik, H.M. Sonawat, Kinetic mechanism of glucose dehydrogenase from *Halobacterium salinarum*, Indian J. Biochem. Biophys. 36 (1999) 143–149.

[49] A. Yokota, K.I. Sasajima, M. Yoneda, Reactivation of inactivated D-glucose dehydrogenase of a *Bacillus* species by pyridine and adenine nucleotides, Agric. Biol. Chem. 43 (1979) 271–278, https://doi.org/10.1080/00021369.1979.10863440.

[50] S.H. Baik, T. Ide, H. Yoshida, O. Kagami, S. Harayama, Significantly enhanced stability of glucose dehydrogenase by directed evolution, Appl. Microbiol. Biotechnol. 61 (2003) 329–335, https://doi.org/10.1007/s00253-002-1215-1.

[51] K.K. Pulicherla, M. Ghosh, P.S. Kumar, K.R.S.S. Rao, Psychrozymes- The next generation industrial enzymes, J. Mar. Sci. Res. Dev. 1 (2011) 1, https://doi.org/10.4172/2155-9910.1000102.

[52] J. Farrell, A. Rose, Temperature effects on microorganisms, Annu. Rev. Microbiol. 21 (1967) 101–120, https://doi.org/10.1146/annurev.mi.21.100167.000533.

[53] P. Messner, Prokaryotic Glycoproteins: unexplored but important, J. Bacteriol. 186 (2004) 2517–2519, https://doi.org/10.1128/JB.186.9.2517.

[54] J. Eichler, M.W.W. Adams, Posttranslational protein modification in Archaea, Microbiol. Mol. Biol. Rev. 69 (2005) 393–425, https://doi.org/10.1128/MMBR.69.3.393-425.2005.

[55] C.M. Szymanski, B.W. Wren, Protein glycosylation in bacterial mucosal pathogens, Nat. Rev. Microbiol. 3 (2005) 225–237, https://doi.org/10.1038/nrmicro1100.

[56] M. Abu-Qarn, J. Eichler, N. Sharon, Not just for Eukarya anymore: protein glycosylation in Bacteria and Archaea, Curr. Opin. Struct. Biol. 18 (2008) 544–550, https://doi.org/10.1016/j.sbi.2008.06.010.

[57] M. Shylaja, H.S. Seshadri, Glycoproteins: an overview, Biochem. Educ. 17 (1989) 170–178, https://doi.org/10.1016/0307-4412(89)90136-2.

[58] Z. Roth, G. Yehezkel, I. Khalaila, Identification and quantification of protein glycosylation, Int. J. Carbohydr. Chem. 2012 (2012) 640923, https://doi.org/10.1155/2012/640923.

[59] S. Yurist-Doutsch, H. Magidovich, V.V. Ventura, P.G. Hitchen, A. Dell, J. Eichler, N-glycosylation in Archaea: on the coordinated actions of *Haloferax volcanii* AglF and AglM, Mol. Microbiol. 75 (2010) 1047–1058, https://doi.org/10.1111/j.1365-2958.2009.07045.x.

[60] C. Ruiz-Canada, D.J. Kelleher, R. Gilmore, Cotranslational and posttranslational N-glycosylation of polypeptides by distinct mammalian OST isoforms, Cell 136 (2009) 272–283, https://doi.org/10.1016/j.cell.2008.11.047.

[61] M. Fröschle, W. Ulmer, K.D. Jany, Tyrosine modification of glucose dehydrogenase from *Bacillus megaterium* Effect of tetranitromethane on the enzyme in the tetrameric and monomeric state, Eur. J. Biochem. 142 (1984) 533–540, https://doi.org/10.1111/j.1432-1033.1984.tb08318.x.

[62] H. Jörnvall, B. Persson, M. Krook, S. Atrian, R. Gonzàlez-Duarte, J. Jeffery, D. Ghosh, Short-chain dehydrogenases/reductases (SDR), Biochemistry 34 (1995) 6003–6013, https://doi.org/10.1021/bi00018a001.

[63] K. Yamamoto, G. Kurisu, M. Kusunoki, S. Tabata, I. Urabe, S. Osaki, Crystal structure of glucose dehydrogenase from *Bacillus megaterium* IWG3 at 1.7 Á resolution, J. Biochem. 129 (2001) 303–309, https://doi.org/10.1093/oxfordjournals.jbchem.a002858.

[64] M.G. Rossman, A. Liljas, C.I. Brändén, L.J. Banaszak, Evolutionary and structural relationships among dehydrogenases, Enzymes 11 (1975) 61–102, https://doi.org/10.1016/S1874-6047(08)60210-3.

[65] J. John, S.J. Crennell, D.W. Hough, M.J. Danson, G.L. Taylor, The crystal structure of glucose dehydrogenase from *Thermoplasma acidophilum*, Structure 2 (1994) 385–393, https://doi.org/10.1016/S0969-2126(00)00040-X.

[66] M.G. Rossmann, D. Moras, K.W. Olsen, Chemical and biological evolution of a nucleotide-binding protein, Nature 250 (1974) 194–199, https://doi.org/10.1038/250194a0.

[67] A. Basner, G. Antranikian, Isolation and biochemical characterization of a glucose dehydrogenase from a hay infusion metagenome, PLoS One 9 (2014) e85844, https://doi.org/10.1371/journal.pone.0085844.

[68] C.A. Bottoms, P.E. Smith, J.J. Tanner, A structurally conserved water molecule in Rossmann dinucleotide-binding domains, Protein Sci. 11 (9) (2002) 2125–2137, https://doi.org/10.1110/ps.0213502.

[69] U. Oppermann, C. Filling, M. Hult, N. Shafqat, X. Wu, M. Lindh, J. Shafqat, E. Nordling, Y. Kallberg, B. Persson, H. Jörnvall, Short-chain dehydrogenases, reductases (SDR): the 2002 update, Chem. Biol. Interact. 143–144 (2003) 247–253, https://doi.org/10.1016/S0009-2797(02)00164-3.

[70] E. Dominguez, L. Gorton, Electrochemistry of NAD(P)+/NAD(P)H, Encycl. Electrochem., vol. 9, in: D.S. Wilson (Ed.), Bioelectrochemistry, Wiley-VCH Verlag, Weinheim, 2002, pp. 67–143.

[71] L. Gorton, E. Dominguez, Electrocatalytic oxidation of NAD(P)H at mediator-modified electrodes, Rev. Mol. Biotechnol. 82 (2002) 371–392.

[72] P.N. Bartlett, L. Gorton, NAD(P) – based biosensors, in: P.N. Bartlet (Ed.), Bioelectrochemistry Fundamentals, Experimental Techniques and Applications, John Wiley & Sons, Chichester, 2008, pp. 157–198.

[73] C.H. Wong, G.M. Whitesides, Enzyme-catalyzed organic synthesis: NAD(P)H cofactor regeneration by using glucose-6-phosphate and the glucose-5-phosphate dehydrogenase from *Leuconostoc mesenteroides*, J. Am. Chem. Soc. 103 (1981) 4890–4899, https://doi.org/10.1021/ja00406a037.

[74] N.J. Oppenheimer, N.O. Kaplan, Structure of the primary acid rearrangement product of reduced nicotinamide adenine dinucleotide (NADH), Biochemistry 13 (1974) 4675–4685, https://doi.org/10.1021/bi00720a001.

[75] C.H. Wong, G.M. Whitesides, Oxidoreductions, in: Enzymes in synthetic organic chemistry 3rd ed., in: C.H. Wong, G.M. Whitesides (Eds.), Elsevier Sc. Ltd., Oxford, pp. 131–194. ISBN 0080359426.

[76] S. Borgmann, G. Hartwich, A. Schulte, W. Schuhmann, Amperometric enzyme sensors based on direct and mediated electron transfer, Perspect. Bioanal. 1 (2005) 599–655, https://doi.org/10.1016/S1871-0069(05)01017-7.

[77] P.N. Bartlett, R.G. Whitaker, Strategies for the development of amperometric enzyme electrodes, Biosensors. 3 (1987) 359–379, https://doi.org/10.1016/0265-928X(87)80018-4.

[78] I. Katakis, E. Dominguez, Catalytic electrooxidation of NADH for dehydrogenase amperometric biosensors, Microchim. Acta 126 (1997) 11–32, https://doi.org/10.1007/bf01242656.

[79] P.N. Bartlett, E. Simon, C.S. Toh, Modified electrodes for NADH oxidation and dehydrogenase-based biosensors, Bioelectrochem. 56 (2002) 117–122, https://doi.org/10.1016/S1567-5394(02)00047-6.

[80] R. Appelqvist, G. Marko-Varga, L. Gorton, A. Torstensson, G. Johansson, Enzymatic determination of glucose in a flow system by catalytic oxidation of the nicotinamide coenzyme at a modified electrode, Anal. Chim. Acta 169 (1985) 237–247, https://doi.org/10.1016/S0003-2670(00)86226-1.

[81] G. Marko-Varga, R. Appelqvist, L. Gorton, A glucose sensor based on glucose dehydrogenase adsorbed on a modified carbon electrode, Anal. Chim. Acta 179 (1986) 371–379.

[82] M. Polasek, L. Gorton, R. Appelqvist, G. Marko-Varga, G. Johansson, Amperometric glucose sensor based on glucose dehydrogenase immobilized on a graphite electrode modified with an N, N'-bis (benzophenoxazinyl) derivative of benzene-1,4-dicarboxamide, Anal. Chim. Acta 246 (1991) 283–292.

[83] B. Persson, H.L. Lan, L. Gorton, Y. Okamoto, P.D. Hale, L.I. Boguslavsky, T. Skotheim, Amperometric biosensors based on electrocatalytic regeneration of NAD^+ at redox polymer-modified electrodes, Biosens. Bioelectron. 8 (1993) 81–88.

[84] Y. Kajiya, H. Matsumoto, H. Yoneyama, Glucose sensitivity of poly(pyrrole) films containing immobilized glucose dehydrogenase, nicotinamide adenine dinucleotide, and β-naphthoquinonesulphonate ions, J. Electroanal. Chem. 319 (1991) 185–194.

[85] U. Bilitewski, P. Ruger, R.D. Schmid, Glucose biosensors based on thick film technology, Biosens. Bioelctron. 6 (1991) 369–373.

[86] A.A. Karyakin, E.E. Karyakina, W. Schuhmann, H.-L. Schmidt, S.D. Varfolorneyev, New amperometric dehydrogenase electrodes based on electrocatalytic NADH-oxidation at poly(methylene blue) modified electrodes, Electroanal. 6 (1994) 821–829.

[87] L.I. Boguslavsky, L. Geng, I.P. Kovalev, S.K. Sahni, Z. Xu, T.A. Skotheim, V. Laurinavicius, B. Persson, L. Gorton, Amperometric thin film biosensors based on glucose dehydrogenase and Toluidine Blue O as catalyst for NADH electrooxidation, Biosens. Bioelectron. 10 (1995) 693–704, https://doi.org/10.1016/0956-5663(95)96960-7.

[88] M. Hedenmo, A. Narvaeza, E. Dorninguez, I. Katakis, Reagent less amperometric glucose dehydrogenase biosensor based on electrocatalytic oxidation of NADH by osmium phenanthrolinedione mediator, Analyst 121 (1996) 1891–1895.

[89] A. Silber, N. Hampp, W. Schuhmann, Poly(methylene blue)-modified thick film gold electrodes for the electrocatalytic oxidation of NADH and their application in glucose biosensors, Biosens. Bioelectron. 11 (1996) 215–223.

[90] A.F. Martin, T.A. Nieman, Chemiluminescence biosensors using tris(2,2'-) ruthenium(II) and dehydrogenases immobilized in cation exchange polymers, Biosens. Bioelectron. 12 (1997) 479–489, https://doi.org/10.1016/S0956-5663(97)00004-3.

[91] D.M. Zhou, J.J. Sun, H.Y. Chen, H.Q. Fang, Electrochemical polymerization of toluidine blue and its application for the amperometric determination of β-D-glucose, Electrochim. Acta 43 (1998) 1803–1809, https://doi.org/10.1016/S0013-4686(97)00297-1.

[92] M. Zhang, A. Smith, W. Gorski, Carbon nanotube-chitosan system for electrochemical sensing based on dehydrogenase enzymes, Anal. Chem. 76 (2004) 5045–5050, https://doi.org/10.1021/ac049519u.

[93] R. Antiochia, I. Lavagnini, P. Pastore, F. Magno, A comparison between the use of a redox mediator in solution and of surface modified electrodes in the electrocatalytic oxidation of nicotinamide adenine dinucleotide, Bioelectrochem. 64 (2004) 157–163, https://doi.org/10.1016/j.bioelechem.2004.01.002.

[94] R. Antiochia, L. Gorton, Development of a carbon nanotube paste electrode osmium polymer-mediated biosensor for determination of glucose in

alcoholic beverages, Biosens. Bioelectron. 22 (2007) 2611–2617, https://doi.org/10.1016/j.bios.2006.10.023.
[95] M. Zhang, C. Mullens, W. Gorski, Coimmobilization of dehydrogenases and their cofactors in electrochemical biosensors, Anal. Chem. 79 (2007) 2446–2450, https://doi.org/10.1021/ac061698n.
[96] Y.M. Yan, O. Yehezkeli, I. Willner, Integrated, electrically contacted NAD(P)$^+$-dependent enzyme-carbon nanotube electrodes for biosensors and biofuel cell applications, Chem. A Eur. J. 13 (2007) 10168–10175, https://doi.org/10.1002/chem.200700806.
[97] P. Du, P. Wu, C. Cai, A glucose biosensor based on electrocatalytic oxidation of NADPH at single-walled carbon nanotubes functionalized with poly(nile blue A), J. Electroanal. Chem. 624 (2008) 21–26, https://doi.org/10.1016/j.jelechem.2008.07.031.
[98] L. Deng, Y. Wang, L. Shang, D. Wen, F. Wang, S. Dong, A sensitive NADH and glucose biosensor tuned by visible light based on thionine bridged carbon nanotubes and gold nanoparticles multilayer, Biosens. Bioelectron. 24 (2008) 951–957, https://doi.org/10.1016/j.bios.2008.07.066.
[99] H. Muguruma, S. Yoshida, M. Urata, K. Fujisawa, Y. Matsui, An amperometric biosensor for glucose based on a composite electrode of glucose dehydrogenase, carbon nanotubes, and plasma-polymerized thin films, Electrochem. 76 (2008) 545–548, https://doi.org/10.5796/electrochemistry.76.545.
[100] A. Hiratsuka, K. Fujisawa, H. Muguruma, Amperometric biosensor based on glucose dehydrogenase and plasma-polymerized thin films, Anal. Sci. 24 (2008) 483–486, https://doi.org/10.2116/analsci.24.483.
[101] H. Zhou, Z. Zhang, P. Yu, L. Su, T. Ohsaka, L. Mao, Noncovalent attachment of NAD$^+$ cofactor onto carbon nanotubes for preparation of integrated dehydrogenase-based electrochemical biosensors, Langmuir 26 (2010) 6028–6032, https://doi.org/10.1021/la903799n.
[102] M. Piano, S. Serban, N. Biddle, R. Pittson, G.A. Drago, J.P. Hart, A flow injection system, comprising a biosensor based on a screen-printed carbon electrode containing Meldola's Blue-Reinecke salt coated with glucose dehydrogenase, for the measurement of glucose, Anal. Biochem. 396 (2010) 269–274, https://doi.org/10.1016/j.ab.2009.09.028.
[103] F.S. Saleh, L. Mao, T. Ohsaka, Development of a dehydrogenase-based glucose anode using a molecular assembly composed of nile blue and functionalized SWCNTs and its applications to a glucose sensor and glucose/O_2 biofuel cell, Sens. Actuators, B Chem. 152 (2011) 130–135, https://doi.org/10.1016/j.snb.2010.07.054.
[104] P. Yu, H. Zhou, H. Cheng, Q. Qian, L. Mao, Rational design and one-step formation of multifunctional gel transducer for simple fabrication of integrated electrochemical biosensors, Anal. Chem. 83 (2011) 5715–5720, https://doi.org/10.1021/ac200942a.
[105] R. Lei, X. Wang, S. Zhu, N. Li, A novel electrochemiluminescence glucose biosensor based on alcohol-free mesoporous molecular sieve silica modified electrode, Sens. Actuators B Chem. 158 (2011) 124–129, https://doi.org/10.1016/j.snb.2011.05.054.
[106] F.S. Saleh, L. Mao, T. Ohsaka, A promising dehydrogenase-based bioanode for a glucose biosensor and glucose/O_2 biofuel cell, Analyst 137 (2012) 2233–2238, https://doi.org/10.1039/c2an15971f.
[107] L. Bai, D. Wen, J. Yin, L. Deng, C. Zhu, S. Dong, Carbon nanotubes-ionic liquid nanocomposites sensing platform for NADH oxidation and oxygen, glucose detection in blood, Talanta 91 (2012) 110–115, https://doi.org/10.1016/j.talanta.2012.01.027.
[108] T. Hoshino, S.I. Sekiguchi, H. Muguruma, Amperometric biosensor based on multilayer containing carbon nanotube, plasma-polymerized film, electron transfer mediator phenothiazine, and glucose dehydrogenase, Bioelectrochem. 84 (2012) 1–5, https://doi.org/10.1016/j.bioelechem.2011.09.001.
[109] D.M. Kim, M.Y. Kim, S.S. Reddy, J. Cho, C.H. Cho, S. Jung, Y.B. Shim, Electron-transfer mediator for a NAD-glucose dehydrogenase-based glucose sensor, Anal. Chem. 85 (2013) 11643–11649, https://doi.org/10.1021/ac403217t.
[110] B. Liang, L. Li, X.J. Tang, Q. Lang, H. Wang, F. Li, J. Shi, W. Shen, I. Palchetti, M. Mascini, A. Liu, Microbial surface display of glucose dehydrogenase for amperometric glucose biosensor, Biosens. Bioelectron. 45 (2013) 19–24, https://doi.org/10.1016/j.bios.2013.01.050.
[111] W. Ma, Q. Jiang, P. Yu, L. Yang, L. Mao, Zeolitic imidazolate framework-based electrochemical biosensor for in vivo electrochemical measurements, Anal. Chem. 85 (2013) 7550–7557, https://doi.org/10.1021/ac401576u.
[112] A. Korani, A. Salimi, Fabrication of high performance bioanode based on fruitful association of dendrimer and carbon nanotube used for design O_2/glucose membrane-less biofuel cell with improved bilirubine oxidase biocathode, Biosens. Bioelectron. 50 (2013) 186–193, https://doi.org/10.1016/j.bios.2013.05.047.
[113] F. Jafari, A. Salimi, A. Navaee, Electrochemical and photoelectrochemical sensing of dihydronicotinamide adenine dinucleotide and glucose based on noncovalently functionalized reduced graphene oxide-cadmium sulfide quantum dots/poly-nile blue nanocomposite, Electroanal. 26 (2014) 1782–1793, https://doi.org/10.1002/elan.201400164.
[114] S.J. Cho, C.-H. Cho, K.B. Kim, M.-H. Lee, J.H. Kim, S. Lee, J. Cho, S. Jung, D.-M. Kim, Y.-B. Shim, Interference reduction in glucose detection by redox potential tuning: New glucose meter development, Anal. Sci. 31 (2015) 705–710, https://doi.org/10.2116/analsci.31.705.
[115] D.G. Dilgin, H.I. Gökçel, Photoelectrochemical glucose biosensor in flow injection analysis system based on glucose dehydrogenase immobilized on poly-hematoxylin modified glassy carbon electrode, Anal. Methods. 7 (2015) 990–999, https://doi.org/10.1039/c4ay02269f.
[116] A. Korani, A. Salimi, H. Hadadzadeh, Nickel-phendione complex covalently attached onto carbon nanotube/cross linked glucose dehydrogenase as bioanode for glucose/oxygen compartment-less biofuel cell, J. Power Sources. 282 (2015) 586–595, https://doi.org/10.1016/j.jpowsour.2015.02.009.
[117] B. Ertek, C. Akgül, Y. Dilgin, Photoelectrochemical glucose biosensor based on a dehydrogenase enzyme and NAD$^+$/NADH redox couple using a quantum dot modified pencil graphite electrode, RSC Adv. 6 (2016) 20058–20066, https://doi.org/10.1039/c5ra25673a.
[118] A. Mahadevan, S. Fernando, Inorganic iron-sulfur clusters enhance electron transport when used for wiring the NAD-glucose dehydrogenase based redox system, Microchim. Acta. 185 (2018) 337, https://doi.org/10.1007/s00604-018-2871-x.
[119] D.G. Dilgin, B. Ertek, Y. Dilgin, A low-cost, fast, disposable and sensitive biosensor study: flow injection analysis of glucose at poly-methylene blue-modified pencil graphite electrode, J. Iran. Chem. Soc. 15 (2018) 1355–1363, https://doi.org/10.1007/s13738-018-1335-x.
[120] Y. Mie, Y. Yasutake, M. Ikegami, T. Tamura, Anodized gold surface enables mediator-free and low-overpotential electrochemical oxidation of NADH: A facile method for the development of an NAD$^+$ - dependent enzyme biosensor, Sens. Actuators B Chem. 288 (2019) 512–518, https://doi.org/10.1016/j.snb.2019.03.039.
[121] A.M.J. Haque, P. Nandhakumar, H. Yang, Specific and rapid glucose detection using NAD-dependent glucose dehydrogenase, diaphorase, and osmium complex, Electroanal. 31 (2019) 1–8, https://doi.org/10.1002/elan.201800814.
[122] J. Wang, Carbon-Nanotube based electrochemical biosensors : A review, Electroanal. 17 (2005) 7–14, https://doi.org/10.1002/elan.200403113.
[123] S.K. Vashist, D. Zheng, K. Al-Rubeaan, J.H.T. Luong, F.-S. Sheu, Advances in carbon nanotube based electrochemical sensors for bioanalytical applications, Biotechnol. Adv. 29 (2011) 169–188, https://doi.org/10.1016/j.biotechadv.2010.10.002.
[124] H.K. Chenault, G.M. Whitesides, Regeneration of nicotinamide cofactors for use in organic synthesis, Appl. Biochem. Biotechnol. 14 (1987) 147–197, https://doi.org/10.1007/BF02798431.
[125] M.J. Lobo, A.J. Miranda, P. Tuñón, Amperometric biosensors based on NAD(P)-dependent dehydrogenase enzymes, Electroanal. 9 (1997) 191–202, https://doi.org/10.1002/elan.1140090302.
[126] L. Gorton, Carbon paste electrodes modified with enzymes, tissues, and cells, Electroanal. 7 (1995) 23–45, https://doi.org/10.1002/elan.1140070104.
[127] L. Gorton, G. Bremle, E. Csoregi, G. Jonsson-Pettersson, B. Persson, Amperometric glucose sensors based on immobilized glucose-oxidizing enzymes and chemically modified electrodes, Anal. Chim. Acta 249 (1991) 43–54.
[128] G. Bremle, B. Persson, L. Gorton, An amperometric glucose electrode based on carbon paste, chemically modified with glucose dehydrogenase, nicotinamide adenine dinucleotide, and a phenoxazine mediator, coated with a poly(ester sulfonic acid) cation exchanger, Electroanal. 3 (1991) 77–86.
[129] T. Ikeda, Bioelectrochemical studies based on enzyme-electrocatalysis, Electrochim. Acta. 82 (2012) 158–164, https://doi.org/10.1016/j.electacta.2012.01.114.
[130] S. Yabuki, H. Shinohara, Y. Ikariyama, M. Aizawa, Electrical activity controlling system for a mediator-coexisting alcohol dehydrogenase-NAD conductive membrane, J. Electroanal. Chem. 277 (1990) 179–187, https://doi.org/10.1016/0022-0728(90)85100-J.
[131] B. Prieto-Simón, E. Fàbregas, Comparative study of electron mediators used in the electrochemical oxidation of NADH, Biosens. Bioelectron. 19 (2004) 1131–1138, https://doi.org/10.1016/j.bios.2003.10.010.
[132] I. Willner, A. Riklin, Electrical communication between electrodes and NAD(P)$^+$-dependent enzymes using pyrroloquinolinequinone-Enzyme electrodes in a self-assembled monolayer configuration: Design of a new class of amperometric biosensors, Anal. Chem. 66 (1994) 1535–1539, https://doi.org/10.1021/ac00081a028.
[133] A. Bardea, E. Katz, A.F. Bückmann, I. Willner, NAD$^+$-dependent enzyme electrodes: Electrical contact of cofactor-dependent enzymes and electrodes, J. Am. Chem. Soc. 119 (1997) 9114–9119, https://doi.org/10.1021/ja971192+.
[134] I. Willner, E. Katz, B. Willner, R. Blonder, V. Heleg-Shabtai, A.F. Bückmann, Assembly of functionalized monolayers of redox proteins on electrode surfaces: novel bioelectronic and optobioelectronic systems, Biosens. Bioelectron. 12 (1997) 337–356, https://doi.org/10.1016/S0956-5663(96)00065-6.
[135] I. Willner, E. Katz, B. Willner, Electrical contact of redox enzyme layers associated with electrodes: Routes to amperometric biosensors, Electroanal. 9 (1997) 965–977, https://doi.org/10.1002/elan.1140091302.
[136] M. Zayats, E. Katz, I. Willner, Electrical contacting of flavoenzymes and NAD(P)$^+$-dependent enzymes by reconstitution and affinity interactions on phenylboronic acid monolayers associated with Au-electrodes, J. Am. Chem. Soc. 124 (2002) 14724–14735, https://doi.org/10.1021/ja027919y.
[137] E. Al-Jawadi, S. Pöller, R. Haddad, W. Schuhmann, NADH oxidation using modified electrodes based on lactate and glucose dehydrogenase entrapped between an electrocatalyst film and redox catalyst-modified polymers, Microchim. Acta 177 (2012) 405–410, https://doi.org/10.1007/s00604-012-0797-2.

[138] J. Pilas, T. Selmer, M. Keusgen, M.J. Schöning, Screen-printed carbon electrodes modified with graphene oxide for the design of a reagent-free NAD-dependent biosensor array, Anal. Chem. 91 (2019) 15293–15299, https://doi.org/10.1021/acs.analchem.9b04481.
[139] G.T.R. Palmore, H. Bertschy, S.H. Bergens, G.M. Whitesides, A methanol/dioxygen biofuel cell that uses NAD^+ - dependent dehydrogenases as catalysts: Application of an electro-enzymatic method to regenerate nicotinamide adenine dinucleotide at low overpotentials, J. Electroanal. Chem. 443 (1998) 155–161, https://doi.org/10.1016/S0022-0728(97)00393-8.
[140] C. Pire, M.L. Camacho, J. Ferrer, D.W. Hough, M.J. Bonete, NAD(P)$^+$-glucose dehydrogenase from *Haloferax mediterranei*: Kinetic mechanism and metal content, J. Mol. Catal. B Enzym. 10 (2000) 409–417, https://doi.org/10.1016/S1381-1177(99)00113-7.
[141] L. Geng, I. Boguslavsky, I.P. Kovalev, S.K. Sahni, H. Kalash, T.A. Skotheim, H.S. Lee, V. Laurinavicius, Amperometric biosensors based on dehydrogenase/NAD and heterocyclic quinones, Biosens. Bioelectron. 11 (1996) 1267–1275.
[142] F. Sato, M. Togo, M.K. Islam, T. Matsue, J. Kosuge, N. Fukasaku, S. Kurosawa, M. Nishizawa, Enzyme-based glucose fuel cell using vitamin K3-immobilized polymer as an electron mediator, Electrochem. Commun. 7 (2005) 643–647, https://doi.org/10.1016/j.elecom.2005.04.015.
[143] Y. Yan, W. Zheng, L. Su, L. Mao, Carbon-nanotube-based glucose/O_2 biofuel cells, Adv. Mater. 18 (2006) 2639–2643, https://doi.org/10.1002/adma.200600028.
[144] A. Korani, A. Salimi, High performance glucose/O_2 compartment-less biofuel cell using DNA/CNTs as platform for immobilizing bilirubin oxidase as novel biocathode and integrated NH_2-CNTs/dendrimer/glucose dehydrogenase/nile blue as bioanode, Electrochim. Acta 185 (2015) 90–100, https://doi.org/10.1016/j.electacta.2015.10.090.
[145] M. Zhou, L. Deng, D. Wen, L. Shang, L. Jin, S. Dong, Highly ordered mesoporous carbons-based glucose/O_2 biofuel cell, Biosens. Bioelectron. 24 (2009) 2904–2908.
[146] D. Wen, X. Xu, S. Dong, A single-walled carbon nanohorn-based miniature glucose/air biofuel cell for harvesting energy from soft drinks, Energy Environ. Sci. 4 (2011) 1358–1363, https://doi.org/10.1039/c0ee00080a.
[147] L. Zhang, M. Zhou, D. Wen, L. Bai, B. Lou, S. Dong, Small-size biofuel cell on paper, Biosens. Bioelectron. 35 (2012) 155–159, https://doi.org/10.1016/j.bios.2012.02.035.
[148] S. Abdellaoui, R.D. Milton, T. Quah, S.D. Minteer, NAD-dependent dehydrogenase bioelectrocatalysis: The ability of a naphthoquinone redox polymer to regenerate NAD, Chem. Commun. 52 (2016) 1147–1150, https://doi.org/10.1039/c5cc09161f.
[149] T. Quah, R.D. Milton, S. Abdellaoui, S.D. Minteer, Bioelectrocatalytic NAD^+/NADH inter-conversion: transformation of an enzymatic fuel cell into an enzymatic redox flow battery, Chem. Commun. 53 (2017) 8411–8414, https://doi.org/10.1039/c7cc03842a.
[150] F. Gao, Y. Yan, L. Su, L. Wang, L. Mao, An enzymatic glucose/O_2 biofuel cell: Preparation, characterization and performance in serum, Electrochem. Commun. 9 (2007) 989–996, https://doi.org/10.1016/j.elecom.2006.12.008.
[151] X. Li, L. Zhang, L. Su, T. Ohsaka, L. Mao, A miniature glucose/O_2 biofuel cell with a high tolerance against ascorbic acid, Fuel cells 9 (2009) 85–91, https://doi.org/10.1002/fuce.200800054.
[152] M. Togo, A. Takamura, T. Asai, H. Kaji, M. Nishizawa, An enzyme-based microfluidic biofuel cell using vitamin K3-mediated glucose oxidation, Electrochim. Acta 52 (2007) 4669–4674, https://doi.org/10.1016/j.electacta.2007.01.067.
[153] T. Miyake, M. Oike, S. Yoshino, Y. Yatagawa, K. Haneda, H. Kaji, M. Nishizawa, Biofuel cell anode: NAD^+/glucose dehydrogenase-coimmobilized ketjenblack electrode, Chem. Phys. Lett. 480 (2009) 123–126, https://doi.org/10.1016/j.cplett.2009.08.075.
[154] X. Wei, J. Liu, Power sources and electrical recharging strategies for implantable medical devices, Front. Energy Power Eng. China. 2 (2008) 1–13, https://doi.org/10.1007/s11708-008-0016-3.
[155] S. Szczesny, S. Jetzki, S. Leonhardt, Review of current actuator suitability for use in medical implants, Conf. Proc.: Ann. Int. Conf. IEEE Eng. Med. Biol. Soc. 1 (2006) 5956–5959.
[156] S. Topcagic, S.D. Minteer, Development of a membraneless ethanol/oxygen biofuel cell, Electrochim. Acta 51 (2006) 2168–2172, https://doi.org/10.1016/j.electacta.2005.03.090.
[157] L. Deng, F. Wang, H. Chen, L. Shang, L. Wang, T. Wang, S. Dong, A biofuel cell with enhanced performance by multilayer biocatalyst immobilized on highly ordered macroporous electrode, Biosens. Bioelectron. 24 (2008) 329–333, https://doi.org/10.1016/j.bios.2008.04.006.
[158] L. Deng, L. Shang, Y. Wang, T. Wang, H. Chen, S. Dong, Multilayer structured carbon nanotubes/poly-L-lysine/laccase composite cathode for glucose/O_2 biofuel cell, Electrochem. Commun. 10 (2008) 1012–1015, https://doi.org/10.1016/j.elecom.2008.05.001.
[159] K. Toma, F. Seshima, A. Maruyama, T. Arakawa, K. Yano, K. Mitsubayashi, Improved performance air bio-battery based on efficient oxygen supply with a gas/liquid highly-porous diaphragm cell, Biosens. Bioelectron. 124–125 (2019) 253–259, https://doi.org/10.1016/j.bios.2018.09.091.
[160] H. Sakai, T. Nakagawa, Y. Tokita, T. Hatazawa, T. Ikeda, S. Tsujimura, K. Kano, A high-power glucose/oxygen biofuel cell operating under quiescent conditions, Energy Environ. Sci. 2 (2009) 133–138, https://doi.org/10.1039/b809841g.
[161] L. Deng, C. Chen, M. Zhou, S. Guo, E. Wang, S. Dong, Integrated self-powered microchip biosensor for endogenous biological cyanide, Anal. Chem. 82 (2010) 4283–4287, https://doi.org/10.1021/ac100274s.
[162] Z. Zhu, Y. Wang, S.D. Minteer, Y.H.P. Zhang, Maltodextrin-powered enzymatic fuel cell through a non-natural enzymatic pathway, J. Power Sources 196 (2011) 7505–7509, https://doi.org/10.1016/j.jpowsour.2011.04.038.
[163] H. Cheng, Q. Qian, X. Wang, P. Yu, L. Mao, Electricity generation from carboxymethyl cellulose biomass: a new application of enzymatic biofuel cells, Electrochim. Acta. 82 (2012) 203–207, https://doi.org/10.1016/j.electacta.2011.11.122.
[164] T. Matsumoto, S. Shimada, K. Yamamoto, T. Tanaka, A. Kondo, Two-stage oxidation of glucose by an enzymatic bioanode, Fuel Cells. 13 (2013) 960–964, https://doi.org/10.1002/fuce.201300124.
[165] K. MacVittie, E. Katz, Self-powered electrochemical memristor based on a biofuel cell-towards memristors integrated with biocomputing systems, Chem. Commun. 50 (2014) 4816–4819, https://doi.org/10.1039/c4cc01540a.
[166] L. Zhang, Y. Wang, C. Ma, P. Wang, M. Yan, Self-powered sensor for Hg^{2+} detection based on hollow-channel paper analytical devices, RSC Adv. 5 (2015) 24479–24485, https://doi.org/10.1039/c4ra14154g.
[167] C.W. Narvaez Villarrubia, F. Soavi, C. Santoro, C. Arbizzani, A. Serov, S. Rojas-Carbonell, G. Gupta, P. Atanassov, Self-feeding paper based biofuel cell/self-powered hybrid μ-supercapacitor integrated system, Biosens. Bioelectron. 86 (2016) 459–465, https://doi.org/10.1016/j.bios.2016.06.084.
[168] A. Koushanpour, M. Gamella, N. Guz, E. Katz, A biofuel cell based on biocatalytic reactions of glucose on both anode and cathode electrodes, Electroanal. 29 (2017) 950–954, https://doi.org/10.1002/elan.201600706.
[169] E. Pinchon, M. Arugula, K. Pant, S. Singhal, Enhancement of electrochemical performance of bilirubin oxidase modified gas diffusion biocathode by porphyrin precursor, Adv. Phys. Chem. 2018 (2018) 4712547, https://doi.org/10.1155/2018/4712547.
[170] A. Korani, A. Salimi, B. Karimi, Guanine/ionic liquid derived ordered mesoporous carbon decorated with AuNPs as efficient NADH and suitable platform for enzymes immobilization and biofuel cell design biosensor, Electroanal. 29 (2017) 2646–2655, https://doi.org/10.1002/elan.201700466.
[171] K. Wu, Y. Zhang, Y. Wang, S. Ge, M. Yan, J. Yu, X. Song, Paper-based analytical devices relying on visible-light-enhanced glucose/air biofuel cells, ACS Appl. Mater. Interfaces. 7 (2015) 24330–24337, https://doi.org/10.1021/acsami.5b07698.
[172] Y. Amao, N. Shuto, Formate dehydrogenase catalyzed CO_2 reduction in a chlorin-e_6 sensitized photochemical biofuel cell, J. Porphyr. Phthalocyanines. 19 (2015) 459–464, https://doi.org/10.1142/s1088424615500406.
[173] T. Miyake, K. Haneda, N. Nagai, Y. Yatagawa, H. Onami, S. Yoshino, T. Abe, M. Nishizawa, Enzymatic biofuel cells designed for direct power generation from biofluids in living organisms, Energy Environ. Sci. 4 (2011) 5008–5012, https://doi.org/10.1039/c1ee02200h.
[174] B. Persson, L. Gorton, G. Johansson, A. Torstensson, Biofuel anode based on D-glucose dehydrogenase, nicotinamide adenine dinucleotide and a modified electrode, Enzyme Microb. Technol. 7 (1985) 549–552.
[175] L.H. Chau, K.C.F. Leung, W.J. Li, Investigation of GDH/laccase enzymes for bioenergy generation systems, in: 2009 IEEE Int. Conf. Mechatronics Autom. ICMA, 2009, pp. 1855. https://doi.org/10.1109/ICMA.2009.5245001.
[176] D. Wen, L. Deng, M. Zhou, S. Guo, L. Shang, G. Xu, S. Dong, A biofuel cell with a single-walled carbon nanohorn-based bioanode operating at physiological condition, Biosens. Bioelectron. 25 (2010) 1544–1547, https://doi.org/10.1016/j.bios.2009.11.007.
[177] M. Karaśkiewicz, E. Nazaruk, K. Zelechowska, J.F. Biernat, J. Rogalski, R. Bilewicz, Fully enzymatic mediatorless fuel cell with efficient naphthylated carbon nanotube-laccase composite cathodes, Electrochem. Commun. 20 (2012) 124–127, https://doi.org/10.1016/j.elecom.2012.04.011.
[178] J.-Y. Wang, P.-C. Nien, C.-H. Chen, L.-C. Chen, K.-C. Ho, A glucose bio-battery prototype based on a GDH/(polymethylene blue) bioanode and a graphite cathode with an iodide/tri-iodide redox couple, Bioresour. Technol. 116 (2012) 502–506, https://doi.org/10.1016/j.biortech.2012.03.083.
[179] N. Ferrer-Miralles, J. Domingo-Espín, J.L. Corchero, E. Vázquez, A. Villaverde, Microbial factories for recombinant pharmaceuticals, Microb. Cell Fact. 8 (2009) 17, https://doi.org/10.1186/1475-2859-8-17.
[180] L. Tang, A.M. Persky, G. Hochhaus, B. Meibohm, Pharmacokinetic aspects of biotechnology products, J. Pharm. Sci. 93 (2004) 2184–2204, https://doi.org/10.1002/jps.20125.
[181] V.T. Chang, M. Crispin, A.R. Aricescu, D.J. Harvey, J.E. Nettleship, J.A. Fennelly, C. Yu, K.S. Boles, E.J. Evans, D.I. Stuart, R.A. Dwek, E.Y. Jones, R.J. Owens, S.J. Davis, Glycoprotein structural genomics: Solving the glycosylation problem, Structure 15 (2007) 267–273, https://doi.org/10.1016/j.str.2007.01.011.
[182] R.J. Sola, K. Griebenow, Effects of glycosylate on the stability of protein pharmaceuticals, J. Pharm. Sci. 98 (2009) 1223–1245, https://doi.org/10.1002/jps.21504.
[183] X. Chang, B. Xu, Y. Bai, H. Luo, R. Ma, P. Shi, B. Yao, Role of N-linked glycosylation in the enzymatic properties of a thermophilic GH 10 xylanase from *Aspergillus fumigatus* expressed in *Pichia pastoris*, PLoS One 12 (2017) e0171111, https://doi.org/10.1371/journal.pone.0171111.
[184] K.M.H. Nevalainen, V.S.J. Te'o, P.L. Bergquist, Heterologous protein expression in filamentous fungi, Trends Biotechnol. 23 (2005) 468–474, https://doi.org/10.1016/j.tibtech.2005.06.002.
[185] H. Aydin, F.C. Azimi, J.D. Cook, J.E. Lee, A convenient and general expression platform for the production of secreted proteins from human cells, J. Vis. Exp. 65 (2012) e4041, https://doi.org/10.3791/4041.

[186] K. Pankiewicz, K. Watanabe, K. Lesiak-Watanabe, B.M. Goldstein, H.N. Jayaram, The chemistry of nicotinamide adenine dinucleotide (NAD) analogues containing C-nucleosides related to nicotinamide riboside, Curr. Med. Chem. 9 (2002) 733–741, https://doi.org/10.2174/0929867024606920.
[187] R.P. Simon, T. Rumpf, V. Linkuviene, D. Matulis, A. Akhtar, M. Jung, Cofactor analogues as active site probes in lysine acetyltransferases, J. Med. Chem. 62 (2019) 2582–2597, https://doi.org/10.1021/acs.jmedchem.8b01887.
[188] M.J. Barber, A.J. Trimboli, S. Nomikos, E.T. Smith, Direct electrochemistry of the flavin domain of assimilatory nitrate reductase: Effects of NAD^+ and NAD^+ analogs, Arch. Biochem. Biophys. 345 (1997) 88–96, https://doi.org/10.1006/abbi.1997.0223.
[189] R.J. Ansell, D.A.P. Small, C.R. Lowe, The interactions of artificial coenzymes with alcohol dehydrogenase and other NAD(P)(H) dependent enzymes, J. Mol. Catal. B Enzym 6 (1999) 111–123.
[190] N.W. Koper, S.A. Jonker, J.W. Verhoeven, C. van Dijk, Electrochemistry of the 9-phenyl-10-methyl-acridan/acridinium redox system; a high potential NADH/NAD^+ analogue, Recl. Trav. Chim. Pays-Bas. 104 (1985) 296–302, https://doi.org/10.1002/recl.19851041106.
[191] P. Hapiot, J. Moiroux, J.M. Savéant, Electrochemistry of NADH/NAD^+ analogues. A detailed mechanistic kinetic and thermodynamic analysis of the 10-methylacridan/10-methylacridinium couple in acetonitrile, J. Am. Chem. Soc. 112 (1990) 1337–1343, https://doi.org/10.1021/ja00160a007.
[192] A. Anne, P. Hapiot, J. Moiroux, J.M. Savéant, Electrochemistry of synthetic analogues of NAD dimers, J. Electroanal. Chem. 331 (1992) 959–970, https://doi.org/10.1016/0022-0728(92)85017-W.